ALMA MATER STUDIORUM
UNIVERSITÀ DI BOLOGNA

ARCHIVIO ISTITUZIONALE
DELLA RICERCA

Alma Mater Studiorum Università di Bologna
Archivio istituzionale della ricerca

Assessment of geometrical and seasonal effects on the natural ventilation of a pig barn using CFD simulations

This is the final peer-reviewed author's accepted manuscript (postprint) of the following publication:

Published Version:
Bovo, M., Santolini, E., Barbaresi, A., Tassinari, P., Torreggiani, D. (2022). Assessment of geometrical and seasonal effects on the natural ventilation of a pig barn using CFD simulations. COMPUTERS AND ELECTRONICS IN AGRICULTURE, 193(February 2022), 1-17 [10.1016/j.compag.2021.106652].

Availability:
This version is available at: https://hdl.handle.net/11585/902978 since: 2022-11-16

Published:

DOI: http://doi.org/10.1016/j.compag.2021.106652

Terms of use:

Some rights reserved. The terms and conditions for the reuse of this version of the manuscript are specified in the publishing policy. For all terms of use and more information see the publisher's website.

This item was downloaded from IRIS Università di Bologna (https://cris.unibo.it/).
When citing, please refer to the published version.

(Article begins on next page)

27 July 2024

Assessment of geometrical and seasonal effects on the natural ventilation of a pig barn using CFD simulations

Marco Bovo[1] *, Enrica Santolini[1], Alberto Barbaresi[1], Patrizia Tassinari[1], Daniele Torreggiani[1]

[1]*Department of Agricultural and Food Sciences – Agricultural engineering (DISTAL), University of Bologna, Viale Fanin 48, 40127 Bologna, Italy*

*** Corresponding author**: marco.bovo@unibo.it

Abstract

Airflow in naturally ventilated barns usually presents high variability with time and it is rather difficult to estimate because of the presence and interaction of the animals. On the other hand, appropriate ventilation is an essential requirement to ensure animal welfare and efficient and sustainable production. In this regard, the computational fluid dynamic simulations represent a powerful and useful tool and, in this paper, CFD simulations are used to investigate and assess the geometrical and seasonal effects on the natural ventilation of an existing pig barn sited in the northern Italy and composed of six wings converging on a central body.

First, the effects of the complex barn geometry on the ventilation parameters have been investigated by outdoor simulations with eight wind scenarios on a closed envelope building model. From these analyses, both the interaction among the different wings and the influence of the surrounding buildings, have been carefully evaluated and a dimensionless parameter, called ventilation rate ratio, has been proposed and applied to the case study barn to assess the effects of the building geometry on the ventilation efficiency.

Then, starting from the statistical analysis of the free-field ventilation at the site, seven additional wind scenarios have been analysed on a different model of the barn, to evaluate the efficiency of indoor natural ventilation during summer and winter seasons, when the most extreme conditions for animal welfare take place. The ventilation resulted very different during the years from season to season, but also presented valuable differences in the same season, from wing to wing. The outcomes of the paper provide useful indications on the present conditions of the structure and they could be used as decision-making information for the management of the livestock building to identify the most favourable pens for the different finishing pig groups at different fattening stages but also for the planning of the most suitable ventilation retrofitting interventions.

Keywords: *Airflow pattern; CFD simulation; Natural ventilation; Pig barn; Ventilation performance; Ventilation rate.*

1. Introduction

Ventilation is a crucial aspect in the livestock buildings since it is fundamental to guarantee a comfortable environment with satisfactory indoor air quality (Saha *et al.*, 2020; Wang, Pan and Li, 2017). In fact, the ventilation is the most efficient way to remove undesirable air pollutants, like harmful gas and dust, and to obtain a comfortable microclimate for the welfare of the animals (Wang, Zhang and Choi, 2018; Yamada *et al.*, 2016). To create an optimal microclimate, the most important indoor environmental parameters to monitor are: air temperature, relative humidity, gas concentration, air velocity, lighting, air pressure, and noise (Vitali *et al.*, 2020; Chantziaras *et al.*, 2020; Rong *et al.*, 2016). The undesirable gas concentrations mostly influencing the air quality in livestock buildings are carbon dioxide (CO_2), carbon monoxide (CO), ammonia (NH_3), methane (CH_4), hydrogen sulphide (H_2S) and nitrous oxide (N_2O) (Choi et al. 2011). Most of these gases are present in low concentrations in the atmosphere, but they can affect both animal welfare and animal production if the concentrations exceed specific thresholds (Tomasello et al. 2019). These aspects are much more important in buildings for intensive animal husbandry where appropriate ventilation is an essential requirement to ensure both animal welfare and efficient and sustainable production.

Past studies have shown that in central Mediterranean countries, peak values of air temperature and relative humidity, in the hot season were largely higher than the upper critical temperature of the thermo-neutral zone of various livestock species (Gonçalves de Oliveira et al. 2021). Moreover, the indoor conditions could be even worse than outdoor, if building geometry and management solutions are not properly designed to reduce the negative effects on animals (Mossad 2009).

To face these aspects, the experimental monitoring can provide useful information on the quality of indoor air in barns, but unfortunately, if they aren't sufficiently prolonged over the time, their outcomes could be strongly dependent on the external action, wind direction and wind magnitude, and have therefore minor usefulness for the design and optimization of the buildings or even for the evaluation of the average ventilation quality over a long period. Moreover, in buildings with a very complex shape, being able to have the representation of the air quality in the whole layout can result very costly both technically and economically (Vitali et al. 2021b). Airflow inside naturally

ventilated animal housing buildings usually has high variability with time and position in the barn and, moreover, it is rather difficult to estimate its effects due to presence of partitions and interaction with the animals (Bjerg et al. 2000).

On the other hand, the computational fluid dynamics (CFD) simulations actually represent a powerful tool, since they can allow to obtain wind-driven solutions for different wind scenarios, and also for the evaluation of the performance of buildings characterized by particular layouts (Liu, Yang and Niu, 2021; Liu *et al.*, 2016; Ji *et al.*, 2008, Liu *et al.*, 2008). Moreover, CFD simulations can allow to plan and evaluate the most suitable ventilation retrofitting interventions for a building.

As for other agro-industrial productive buildings (Teitel and Wenger, 2014; Kim *et al.*, 2017; Espinoza *et al.*, 2017), the CFD simulations allow to understand in detail both the outdoor airflow and the wind-driven indoor ventilation flow of a building providing the features of the interaction between different buildings as in (King et al. 2017) and useful indication for the management of vents and openings (Jackson *et al.*, 2020; Chu and Lan, 2019).

In the present paper, the CFD analysis have been adopted to investigate and evaluate the geometrical effects and seasonal variations (in terms of wind speed and direction) in a naturally ventilated pig barn, selected as a case study, characterized by a complex layout similar to a six-pointed “star”. In fact, the building is composed of six long wings, oriented in different ways, converging to a central body. After some detailed building surveys, allowing the definition of the geometrical model including both the investigated building and the surrounding facilities, eight wind-driven analyses have been applied along different wind directions in order to obtain indications on both interactions among the wings of the barn and assess the influence of the surrounding facilities, better detailed in the next section. In this regard, a dimensionless parameter called ventilation rate ratio, measuring in a simplified way the effects of the building geometry on the ventilation efficiency, has been proposed in the present paper and calculated for the case study barn. Finally, the natural ventilation efficiency, during the warm and cold seasons of the year has been estimated in terms of indoor air velocity and ventilation rate obtained for each season as a combination based on the statistical analysis of the free-field ventilation at the site. The results

obtained in this paper do not reflect the actual indoor ventilation conditions in the barn chosen as a case study, since the simulations have been run under conditions aimed at focusing on the effects of the structural characteristics of the barn with a more general validity, without taking into account particular conditions about window opening varying daily based on management choices. However, the barn has been selected as an interesting case study because of the complex layout of the building, since it includes parts with different orientations and then represents a situation occurring in several real cases. Moreover, the building is a valuable case where to investigate both the effects of the different orientation and the presence of surrounding buildings with heterogeneous characteristics.

2. Materials and Methods

2.1 Description of the case study

The building is an existing pig barn, located in northern Italy (Latitude=44.9163°, Longitude=10.8817° and Altitude= +25.0m a.s.l.), in a geographical area characterized by hot climate conditions. The barn was originally designed to host dairy cows but in the nineties has been restored and converted to house finisher pigs from about 40-50 kg to about 140-160 kg.

The complex plan layout of the case study building, similar to a “star” with six wings, named w1-w6, is showed in Figure 1 together with some photos, both external and internal.

The central core of the barn, used as a storehouse, has a heptagon shape with edge dimension about 20.0 m, inner height 7.5 m at the eaves and 12.0 m at the top of the center dome. The six wings of the building have length equal to 72.3 m and different width: wings w4 and w5 are wide 19.8 m, whereas w1, w2, w3, and w6 are 17.7 m wide. Their inner height is 3.50 m at the eaves and about 6.20 m at the center (the pitch slope is about 13%). They have partially slatted floor (where 50% is slatted floor and 50% is solid floor) and a central service corridor of about 0.90m which runs along the whole length of the wing. The wings of the building are naturally ventilated with lateral and roof openings. The lateral openings, continuous along the longitudinal sides, have net height of 0.90m

starting from a level of 2.50m measured from the inner pavement. The roof openings are 0.85m high. The wings are connected to the center dome by a closed doors and so each wing is ventilated separately from the others. They are divided in several pens, with typical dimensions 3.3 m × 8.2 m.

(a)

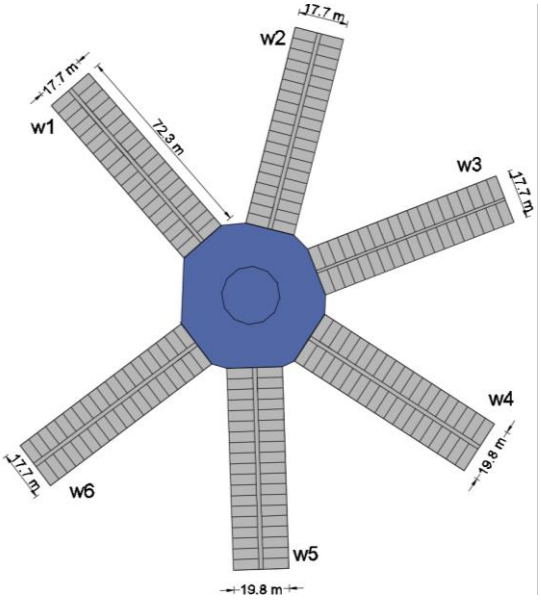

(b)

(c)

(d)

(e)

Figure 1. The case study building. (a) Aerial view; (b) Plan view of the layout; (c) External view; (d) Corridor view and (e) pen view in the wing w3.

2.2 CFD model

Two 3D models have been performed in Autodesk Inventor (Autodesk 2020). In the first model (model A), the pig barn and the surrounding buildings have been modelled as closed envelope buildings (i.e. without openings), as shown in Figure 2c. In the second model (model B), the pig barn has been modelled with its roof and lateral wall openings, as it actually appears (see Figure

2d). The model A has been carried out to simulate a virtual pure outdoor condition useful to provide information on the fluid dynamic interaction between different wings of the barn and also between the barn and the surrounding structures. Model B has been used to assess the actual ventilation conditions of the barn under specific seasonal conditions. The inner walls between the pens and those of the corridor have been modelled as impervious obstacles in their exact position and real geometry. The simulations have been performed with the software Vento AEC (CSPFea 2020). The computational domain, as shown in Figure 2, centred in the pig barn, has dimensions 1050 m × 850 m × 72 m, determined from the height of the pig barn, i.e., H=12m. The distance from the buildings (inscribed in the red rectangle in Figure 2a) to the possible inlet/outlet surfaces has been set to be higher than 25 times the height H of the highest building (Tominaga et al. 2008). The distance to the top of the domain is 5 times H as shown in Figure 2b.

2.2.1 Numerical method and mesh definition

The standard k − ε turbulence model (Launder and Spalding 1983) has been used in CFD simulations to solve the turbulent transport. This model has been selected since stable and widely validated in applications characterized by limited pressure gradients (Richards and Hoxey 1993). The simulations have been conducted under steady state and incompressible conditions. Then, the mass conservation in Eq. (1), momentum conservation in Eq. (2), energy conservation in Eq. (3) and turbulence equations, i.e. Eqs. (4a)-(4b), adopting Einstein's summation notation, are:

$$\frac{\partial u_i}{\partial x_i} = 0 \tag{1}$$

$$u_j \frac{\partial u_i}{\partial x_j} = -\frac{1}{\rho}\frac{\partial p}{\partial x_i} + \frac{\partial}{\partial x_j}\left((\mu + \mu_t)\frac{\partial u_i}{\partial x_j}\right) + \rho g_i + S_U \tag{2}$$

$$u_j \frac{\partial T}{\partial x_j} = \frac{\partial}{\partial x_j}\left(\alpha \frac{\partial T}{\partial x_j}\right) + S_T \tag{3}$$

$$\rho u_j \frac{\partial k}{\partial x_j} = \frac{\partial}{\partial x_j}\left(\left(\mu + \frac{\mu_t}{\sigma_k}\right)\frac{\partial k}{\partial x_j}\right) + \mu_t \left(\frac{\partial u_j}{\partial x_i} + \frac{\partial u_i}{\partial x_j}\right)\frac{\partial u_i}{\partial x_j} - \rho\varepsilon + S_k \tag{4a}$$

$$\rho u_j \frac{\partial \varepsilon}{\partial x_j} = \frac{\partial}{\partial x_j}\left(\left(\mu + \frac{\mu_t}{\sigma_\varepsilon}\right)\frac{\partial \varepsilon}{\partial x_j}\right) + C_{1\varepsilon}\frac{\varepsilon}{k}\mu_t \left(\frac{\partial u_j}{\partial x_i} + \frac{\partial u_i}{\partial x_j}\right)\frac{\partial u_i}{\partial x_j} - \rho C_{2\varepsilon}\frac{\varepsilon^2}{k} + S_\varepsilon \tag{4b}$$

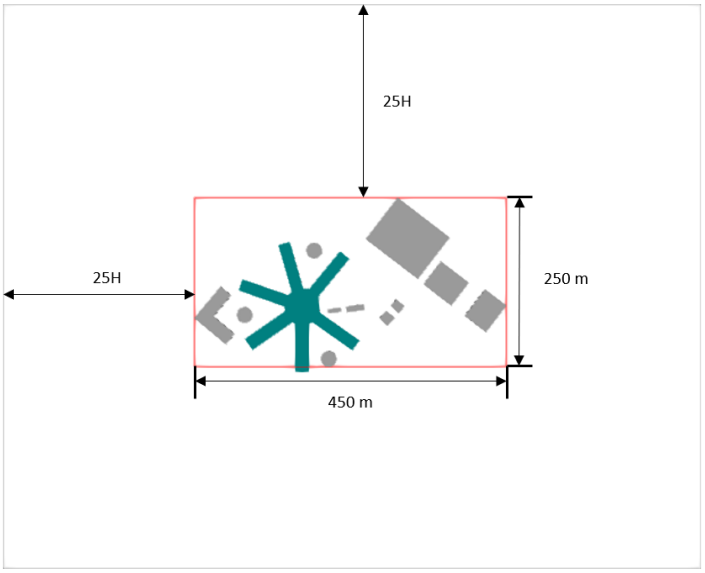

(a)

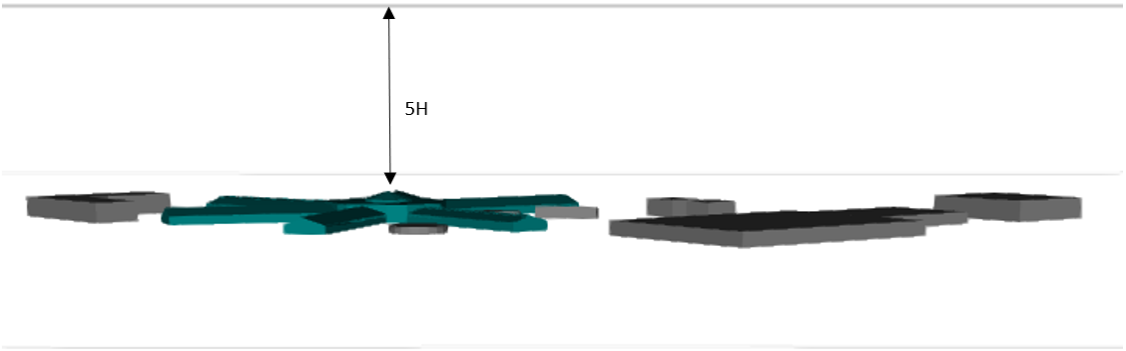

(b)

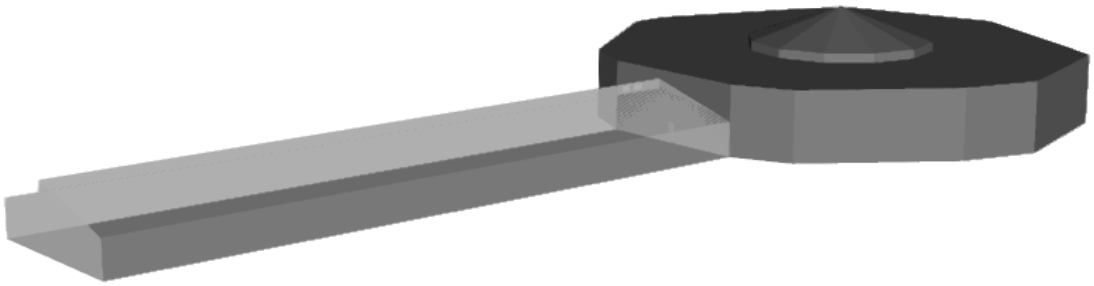

(c)

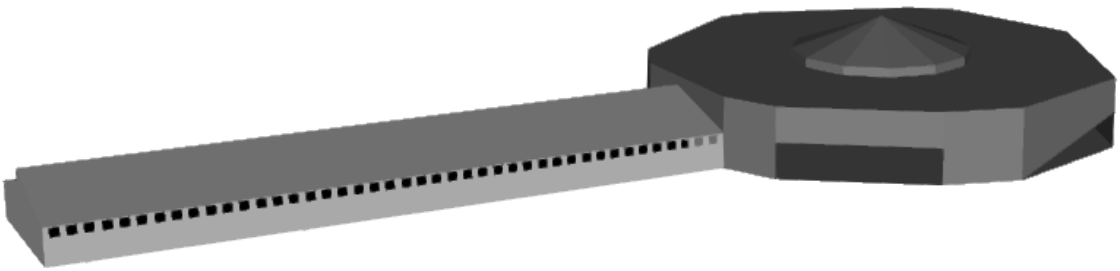

(d)

Figure 2. Geometrical models used in the CFD simulations. (a) Plan view of the domain and (b) lateral view of the domain, where H is the height of the tallest building in the model. (c) Particular of the model A without openings; (d) Particular of the model B with openings.

Where u_j is the velocity components [m s^{-1}]; x_i is the spatial coordinate [m]; p is the pressure [Pa]; ρ is the air density [kg m^{-3}]; μ is air viscosity [m^2 s^{-1}]; μ_t is turbulent (eddy) viscosity, [m^2 s^{-1}]; g_i is the gravitational acceleration [m s^{-2}]; α is thermal diffusivity [m^2 s^{-1}]; k is turbulent kinetic energy [m^2 s^{-2}]; ε is turbulent kinetic energy dissipation [m^2 s^{-3}]; σ_k, σ_ε, $C_{1\varepsilon}$ and $C_{2\varepsilon}$ are constants assumed equal to 1.0, 1.3, 1.44 and 1.92 as suggested in (Richards and Hoxey 1993). S_U, S_T, S_k and S_ε are user definable source terms. For the convergence process, the second order symmetric scheme (Yee 1987) has been chosen and the convergence criteria have been defined for a value equal to 10^{-5} for all field variables.

The software works with Immersed Boundary technique (Huang and Tian 2019) allowing to generate mesh in fast and easy way, even for complicate geometries (Tu, Yeoh, and Liu 2018). The grid convergence study has been conducted based on four different structured meshes, for both the two configurations under study (i.e., closed envelope and open envelope). The meshes have been progressively refined from 2×10^6 to 6×10^6 cells for the closed envelope configuration and from 6×10^6 to 16×10^6 cells for the open envelope configuration. The grid convergence study have considered several velocity profiles extracted from the results of the simulations at a different level above the ground level. In the case of models A, the velocity profiles have been extracted covering the whole domain. Two have been selected very close to the buildings and other two by intersecting the buildings at three different levels. Similar procedure has been followed for the models B, but in this case the profiles extracted also considered indoor areas of the barn. These air velocity (*v*) profiles have been used to evaluate the variation of the results based on the mesh refinement, by means of calculation of the infinity norm, as presented in Eq. (5), progressively from the coarser to the finest mesh:

$$\left|\left|v\right|\right|_\infty = max\,|v_a - v_b| \tag{5}$$

Where *a* refers to the single air velocity vector of the finer mesh and *b* refers to the single air velocity vector of the coarser mesh. The average of the infinity norm, resulting from the comparison of each profile considered, has been calculated, allowing to define the proper grid dimension.

In Figure 3, the results obtained on the meshes for the barn with open envelope configuration, are showed. For the open envelope configuration, the mesh with 8×10^6 cells has been selected for the analyses. For the closed envelope configuration the mesh with 4×10^6 cells has been adopted.

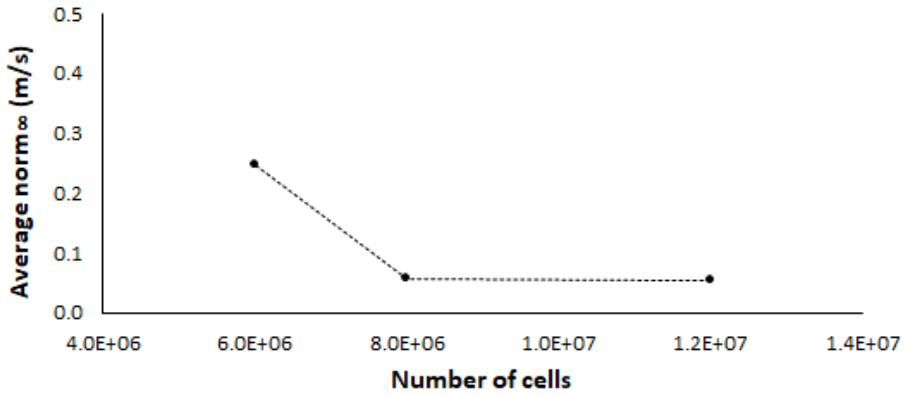

Figure 3. Results of the grid convergence study for the open envelope configuration of the pig barn.

2.2.2 Boundary conditions

Inlet boundary conditions account for the upstream aerodynamic roughness length and describe the vertical profiles for mean velocity and turbulence properties. In all simulations, the wind profile *u(z)*, the kinetic energy *k(z)*, and the dissipation rate *ε(z)* have been defined, assuming constant stress with level (Ramirez, Afshari, and Norford 2018) in the following way:

$$u(z) = \frac{u_*}{\kappa}\, ln\left(\frac{z}{z_0}\right) \tag{6}$$

$$k(z) = \frac{{u_*}^2}{\sqrt{C_\mu}} \tag{7}$$

$$\varepsilon(z) = \frac{{u_*}^3}{\kappa\sqrt{z + z_0}} \tag{8}$$

Where u_* is the friction velocity [m s^{-1}]; κ is the von Karman's constant assumed equal to 0.40; C_μ is a constant, generally assumed equal to 0.09, and z_0 is the ground roughness length [m]. The ground roughness has been set equal to 0.01 m (i.e., open grassland), because the case study farm is

sited in an isolated area in the countryside (see Figure 1). Table 1 collects all the input values and constant values assumed in the numerical simulations.

2.2.3 Model A and scenarios for geometrical effects assessment (SG)

The simulations for the evaluation of the geometrical effects, due to the complex layout of the barn, based on the model A, have been performed under eight scenarios (SG1-SG8), characterized by eight different wind directions, i.e. North, North-East, East, South-East, South, South-West, West and North-West, but homogeneous wind velocity magnitude and air temperature (equal to 20°C). The wind velocity equal to 1.0 m/s at 10.0 m from ground level (g.l.), i.e. $u(10.0) = 1.0$ m/s, has been used to determine the wind profile applied as boundary condition and the friction velocity value (Richards and Hoxey 1993) for the inlet boundaries profiles (Eq. (6), (7) and (8)). The simulations have been focused on the geometrical effects of the layout of the building under different wind directions.

Table 1

Constant and input values assumed in the numerical simulations.

Simulation type	Stead-state condition
Turbulence model	Standard k-ε model
Wind profile	Logarithmic profile
Friction velocity (m/s)	0.23
Von Karman's constant	0.41
Air temperature (°C)	20.0

2.2.4 Model B and scenarios for seasonal effects assessment (SS)

The simulations for the seasonal effects of natural ventilation on the pig barn have been performed based on a statistical analysis of the typical blowing wind at the site of the building during the year. The data have been collected by the weather registration station of Arpae (Emilia Romagna region 2020) named “Rolo”, located only 3.47 km from the pig barn. The analysis has been performed on the hourly prevalent wind direction data and hourly average velocity magnitude data, at 10.0 m above ground level, collected for the solar years 2017, 2018 and, 2019. The analysis has been focused on two seasons characterized by more critical and extreme environmental conditions in terms of indoor climate and animal welfare: the warm season (assumed from June to August) and the cold season (assumed from December to February). Firstly, the percentage of hours in the considered period with wind blowing from a specific direction have been evaluated (see Figure 4 (a1) and 4 (b1)). Then, for each season and for every direction, the hourly average wind velocity magnitude has been calculated, as shown in Figure 4 (a2) and Figure 4 (b2). The average velocity at 10.0 m from g.l. has been considered for the friction velocity determination (Richards and Hoxey 1993).

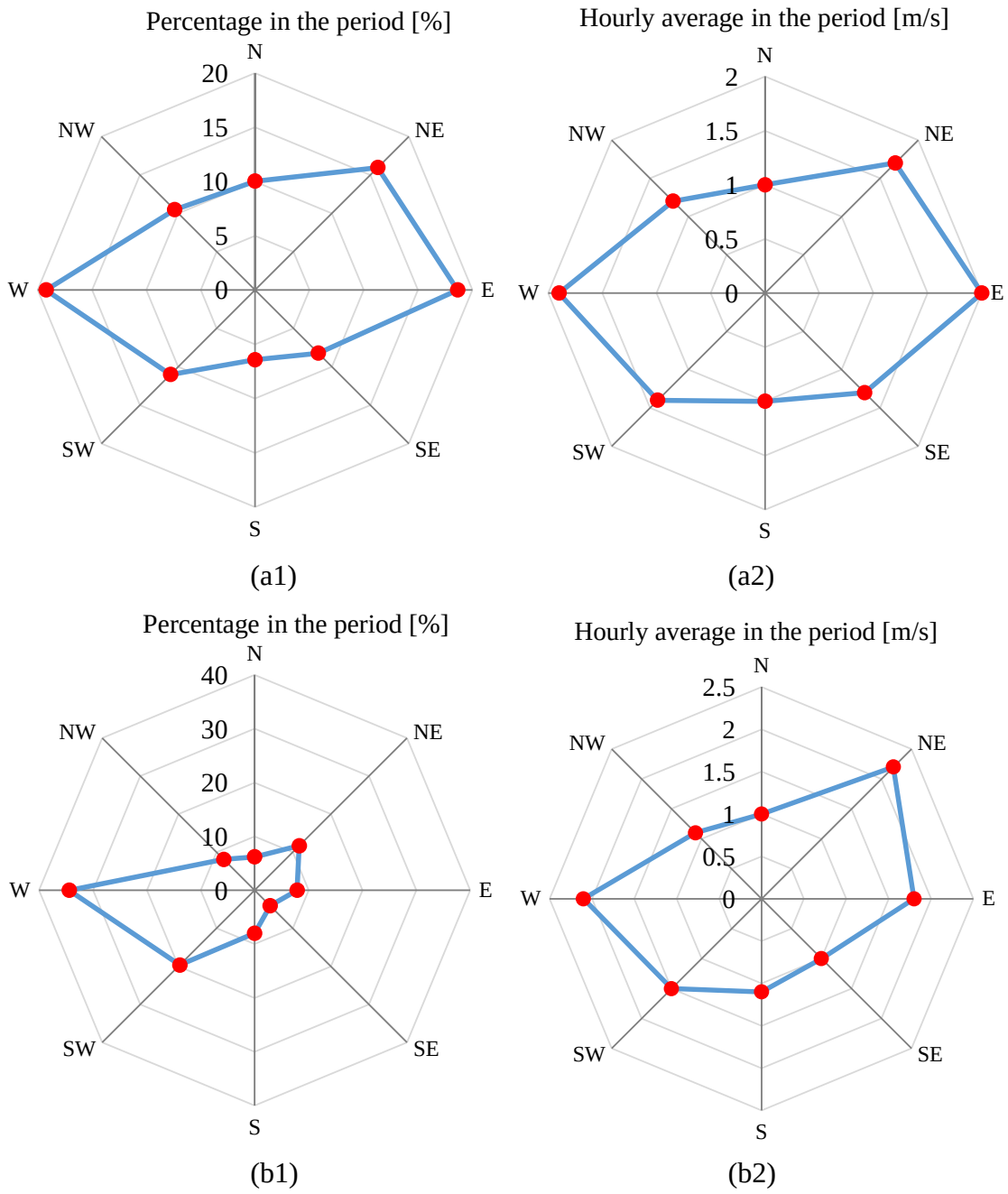

Figure 4. Statistical analysis of the wind conditions in the proximity of the pig barn. Warm season: (a1) percentage and (a2) hourly average velocity magnitude at 10.0m from g.l., in the considered period and with wind blowing in a specific direction. Cold season: (b1) percentage and (b2) hourly average velocity magnitude at 10.0m from g.l., in the considered period, and with wind blowing in a specific direction.

These percentage occurrence of the different wind directions, with their averaged velocity magnitude have been calculated and reported in Table 2. The scenarios investigated have been selected in order to consider at least 65% of the total hours of the two periods (i.e., the two seasons).

The average velocity at 10.0m from g.l. has been considered for the friction velocity determination (Richards and Hoxey 1993).

Table 2

Main outcomes of the statistical analysis of the outdoor conditions as resulting from the data collected by the weather station "ROLO" located in the proximity of the pig barn.

Warm season								
Scenario		**SS3**	**SS2**			**SS4**	**SS1**	
Wind direction	N	**NE**	**E**	SE	S	**SW**	**W**	NW
Average velocity at 10m g.l. (m/s)	1.0	**1.7**	**2.0**	1.3	1.0	**1.4**	**1.9**	1.2
Percentage occurrence (%)	10.0	**16.1**	**18.6**	8.2	6.4	**11.1**	**19.2**	10.5
Air Temperature (°C)	24.8	**25.2**	**25.1**	24.9	25.2	**25.5**	**24.7**	24.7
Cold season								
Scenario		**SS7**				**SS6**	**SS5**	
Wind direction	N	**NE**	E	SE	S	**SW**	**W**	NW
Average velocity at 10m g.l. (m/s)	1.0	**2.2**	1.8	1.0	1.1	**1.5**	**2.1**	1.1
Percentage occurrence (%)	6.2	**11.7**	7.9	4.1	8.0	**19.7**	**34.4**	8.1
Air Temperature (°C)	3.2	**3.4**	3.2	3.6	3.7	**3.8**	**3.5**	3.3

For each SS scenario, based on the wind directions, the average air temperature has been determined on the basis of the hourly average data of the same weather station. So, four different wind scenarios (i.e., SS1 – SS4) have been considered to represent the warm season and three scenarios (i.e., SS5-SS7) have been adopted for the cold season.

2.3 Ventilation performance indicators

The key purpose of an indicator is to investigate what, and in what form, wind environment information is needed to guide design and management so as to achieve better wind penetration, and hence, obtain a better ventilation of the building (Yim et al. 2009). In the present work three performance indicators have been adopted and considered:

- air velocity magnitude (v) at a reference level;
- ventilation rate (Q);
- ventilation rate ratio (Q_R).

The first two indicators are commonly used for the determination of the ventilation efficiency in buildings (Rong et al. 2016). Instead, the ventilation rate ratio Q_R, proposed by the authors in this study, allows to evaluate the effects of building geometry in case of wind-driven ventilation, by

taking into account also the conformation of the surrounding environment. This general purpose indicator has been defined with the main aim to provide, even if in a simplified way, the ventilation efficiency of buildings with complex layout.

2.3.1 Ventilation rate Q

The formulation of the air ventilation rate is based on the wind-driven ventilation mechanism and is suitable in case of negligible, or in absence of effects for stack mechanism (or buoyancy-driven mechanism), as for the building investigated in this paper (Swami and Chandra 1987). The expression of *Q* has been derived starting from a pressure-based methodology used for calculating natural ventilation in buildings by means of an empirical formulation (CIBSE, 2015; Troy Halsey, 2010; (Halsey 2010) and using the average façade pressure coefficients (C_p):

$$C_p = \frac{\Delta P}{\frac{1}{2}\rho U_b^2} \tag{9}$$

where ΔP is the pressure difference between an upwind position and the façade [Pa]; ρ is the fluid density [kg m^{-3}]; U_b represents the upstream basic wind velocity at a certain reference level, typically corresponding to building height at the eaves [m s^{-1}].

Then, the air ventilation rate *Q*, in the case of a single-side open wall, is then nominally calculated starting from the openings area *A* and with the proper discharge coefficient C_d as follows:

$$Q = A\, C_d \sqrt{\frac{2\,\Delta P}{\rho}} \tag{10}$$

where the discharge coefficient C_d is usually experimentally (Iqbal et al. 2015) obtained and for the openings of the case study investigated here, it ranges from 0.66 to 0.67. A similar formulation is available for the evaluation of the air ventilation rate for buildings with wind-induced cross-ventilation that usually occurs in buildings with double-side open walls. The cross-ventilation is due to the static pressure difference across opposite openings in the building (Karava *et al.*, 2011; Golubić *et al.*, 2020) and when the openings have the same area, the ventilation rates *Q*, entering and spilling, can be calculated with the expression (Chu et al. 2017):

$$Q = \frac{1}{\sqrt{2}} C_d A U_b \sqrt{C_{pw} - C_{pl}} \quad (11)$$

Where: C_{pw} is the pressure coefficient on the windward wall and C_{pl} is the equivalent but on the leeward wall. The assessment of C_{pw} and C_{pl} should be accurate and they can be obtained in an experimental or numerical way (Costola, Blocken, and Hensen 2009). Significant efforts have been made to set and implement databases of C_p values for different geometrical conditions and building exposures (Meng et al. 2018), which nowadays are extensively used in building energy simulations and airflow network tools. In this study, considering the peculiar geometry of the building and the correlated effects on the ventilation, the pressure coefficients, C_{pw} and C_{pl}, have been estimated through the CFD simulations. The approximate approach reported here for the assessment of Q can be used in case the values of *Cpw* and *Cpl* are available for the building. In alternative the value of Q can be derived by integrating the normal velocity vectors over the opening surfaces. The first approach can be used in case closed envelope models are adopted (e.g. the case of the Model A in this work) whereas the second approach is viable in case openings are introduced in the models (e.g. the case of the Model B in this work). As far as the building investigated here is concerned, the value of Q can be calculated for each wing for every scenario and the ventilation rate itself could be a useful measure to evaluate if the air exchange, in the volume, is suitable for the intended use of the building or a portion of the building (e.g. a single wing of the case study investigated here).

2.3.2 Ventilation rate ratio, Q_R

The ventilation rate ratio, Q_R, has been defined as ratio of the ventilation rate of the building under study and an equivalent building (reference building) with analogous dimensions and opening area, under any ventilation scenario (*j-th*):

$$Q_R = \frac{Q_j}{Q_{ref,j}} \quad (12)$$

where: Q_j is the ventilation rate of a building in the *j*-th scenario and $Q_{ref,j}$ is the ventilation rate of the reference building in the same scenario. The real ventilation rate of the building under study, Q_R, is normalized to the ventilation rate of a reference building. This parameter has been defined in

order quantify the reduction of the ventilation efficiency for a building with complicated geometry, taking into account all listed aspects, compared to a simple equivalent ventilated building, under the same conditions. It has been developed for building with ventilation openings not facing perpendicularly the incoming wind, due to the peculiar structure geometry.

In this case study, the pig barn is a cross-ventilated building and so the ventilation rate has been defined based on Eq. (11), where the values of C_{pw} and $C_{pl,}$ have been obtained via CFD simulations as average values calculated over the opening area A, in each of the ventilation scenarios investigated. Then, the ventilation rate, $Qref,_j$ (Eq. (11)), of the reference building has been calculated as the ventilation rate of a cross-ventilated building, having parallelepiped geometry with a volume equal to the volume circumscribing the investigated building and with opening area, A_{ref}, analogous to the one of the investigated building, facing perpendicularly the wind (see Figure 5).

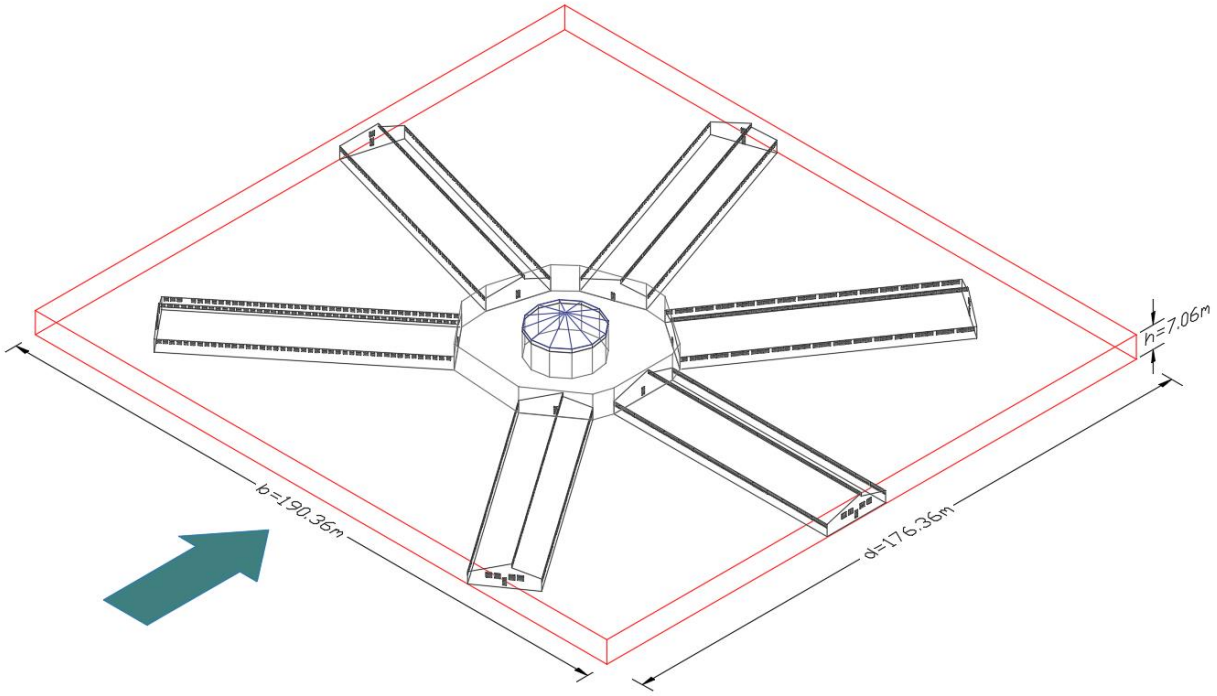

Figure 5. Example of definition of the reference building (red line) based on the pig barn geometry.

From the dimensions (b×d×h) of the reference building, the relative pressure coefficients $C_{pw,}$ and C_{pl} can be derived by methodology available in international building codes (CEN 2010). The methodology proposed by Italian Research Center (CNR 2019) has been used (see Figure 6).

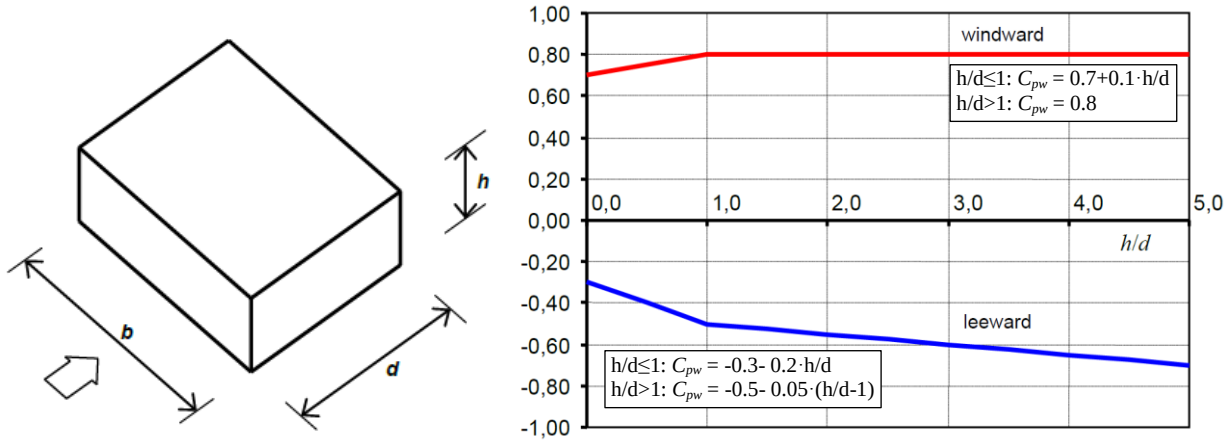

(a) (b)

Figure 6. Calculation of C_{pw} and C_{pl} for windward and leeward walls, respectively. (a) Identification of the values of b, d, h. (b) Trends of the different C_p for different h/d ratio.

When the opening area of the reference building, A_{ref} is assumed equal to area of the real building, A, at the same condition, in a *j-th* scenario, the ventilation rate ratio, Q_R, can be simplified as:

$$Q_{R,j} = \left(\frac{\overline{C_{pw,J} - C_{pl,J}}}{\overline{C_{pw,ref,J} - C_{pl,ref,J}}}\right)^{0.5} \quad (13)$$

Where the symbol (¯) must be intended as average value over the openings area. This proposed parameter represents just an attempt to define a performance index that takes into account the geometry effects and the interaction effects with other bodies in evaluating the ventilation efficiency of a building with generic layout.

2.4 Experimental test

An experimental campaign has been conducted in the wing w3 of the investigated pig barn, empty during the experimental test, in order to collect data not affected by the animal presence. Experimental data on indoor air velocity magnitude have been collected by means of 18 hotwire anemometers (Delta Ohm with accuracy ±0.01m/s) to validate the CFD model. Inside the available wing w3, the data have been collected in six different pens: two at the beginning of the wing, two in

the center and two at the other extremity of the wing. In each selected pen, the air velocity has been detected at 1.0 m of level, in three different positions: one close to the lateral wall in the slatted pavement area, one at the center of the pen and one close to the central corridor, as shown in Figure 7. Therefore, 18 indoor positions have been experimentally selected and investigated by positioning an anemometer in each point. The experimental data on outdoor air velocity (i.e. direction and magnitude) have been acquired during the campaign by means of a ultrasonic anemometer (Delta Ohm with accuracy ±0.01m/s) installed in the close proximity of the pig barn at 3.0m from the ground level.

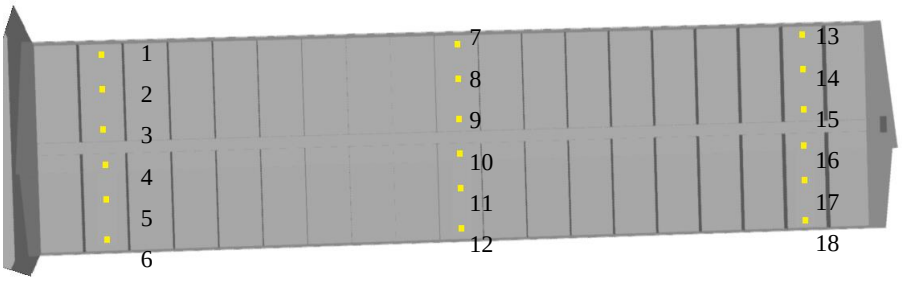

Figure 7. Position of the 18 experimental points in the wing w3 used for the model validation process.

The indoor and outdoor air velocity data have been acquired for 5 minutes using a time step period for the acquisition equal to 2 seconds, for a total of 150 measurements for each point. So, for each one of the experimental point (i.e. 18 indoor points + 1 outdoor point), a dataset of contemporary measures of indoor velocity magnitude and outdoor wind magnitude and direction has been collected. Then, for each experimental point, the average indoor air velocity and the average outdoor air velocity, have been computed. Finally, each one of the 18 indoor average velocity values has been compared to the air velocity provided, in the same position, by the CFD simulation run under the boundary conditions obtained by the elaboration of the outdoor data collected during the experimental campaign (i.e. average wind velocity and predominant wind direction). Figure 8 shows the results of the average indoor air velocity (labelled "*measurements*" in the figure) in the 18 experimental points of the investigated wing of the barn. The whiskers in the figure indicate the

standard deviation values of the air velocity data collected during the test. The results of the validation process are shown in the following section.

3. Results and Discussion

3.1 Validation of the numerical model

The experimental campaign described above has been considered for the validation of the numerical model of the barn. Consistently, with the experimental campaign, in the numerical models adopted in the study the animals and their interaction with the indoor ventilation, have not been considered. From the application of the outdoor wind conditions, to the numerical model B of the barn, the air velocity in the 18 indoor experimental points, described before, have been obtained by means of a CFD simulation. Therefore, the average (experimental) air velocity for each experimental point has been compared to the air velocity provided in the same position by the CFD simulation. The results of the validation process are shown in Figure 8 where experimental and numerical results have been overlapped. The comparison shows limited differences between the experimental measurements and the numerical outcomes. In fact, some numerical results are extremely close to the measured values, such as for point #1, 2, 5, 8, 10, 11, 13, 15 and 17, while the others are placed within the validity range defined by measurement standard deviation, with the only exception of point #12 (see Figure (a.2)). The good fit between model results and experimental outcomes are confirmed by a very low value of the relative mean square error (RMSE) resulting equal to 0.002 m/s.

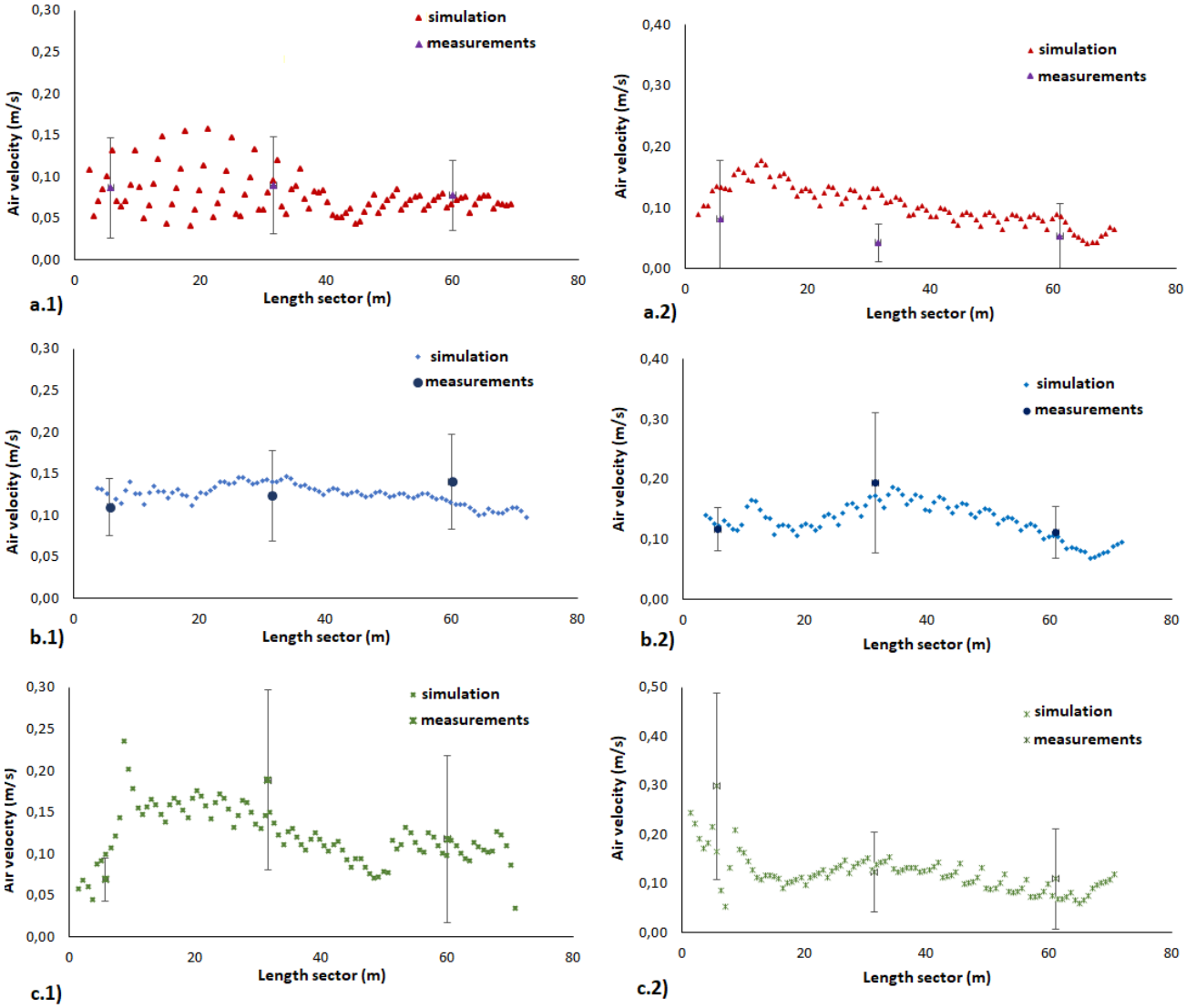

Figure 8. Comparison between the results of CFD simulation and experimental measurements (see Figure 7 for the position of the experimental points). (a.1) section for the points #1, #7 and #13; (a.2) section for the points #6, #12 and #18; (b.1) section for the points #2, #8 and #14; (b.2) section for the points #5, #11 and #17; (c.1) section for the points #3, #9 and #15; (c.2) section for the points #4, #10 and #16.

3.2 Geometrical effects evaluation

3.2.1 Velocity patterns

The air velocity contours for the results of the scenarios from SG1 to SG8 in model A are shown in Figure 9. The direction of the blowing wind in the different scenarios, i.e. the boundary condition considered in the CFD simulation, are represented by the light blue arrows in the figure. As expected, the surrounding buildings affect the wind actions in different ways. For example, in SG1, SG5, and SG6, the surrounding buildings have a negligible effect on the incoming air flow in

relation to the barn structure. However, the wind flow variation is mainly due to the complex geometry of the barn, because in every scenario, the windward wings in such a way block or modify the air flow on the leeward wings. W4, w5, and w6 are in a negative condition (i.e., blowed by a very low magnitude air velocity) in SG1 and vice versa w1, w2, and w3 in SG5. Moreover, also in SG2 and SG4 the surrounding buildings have marginal effects. In particular, SG2 and SG4 show a favoured condition for two specific wings of the barn: w2 and w3 for SG2 and w4 and w5 for SG4. In fact, they are subject to the maximum wind velocity, equal to 2 m/s, due to the absence of surrounding buildings or barn wings acting as obstacles.

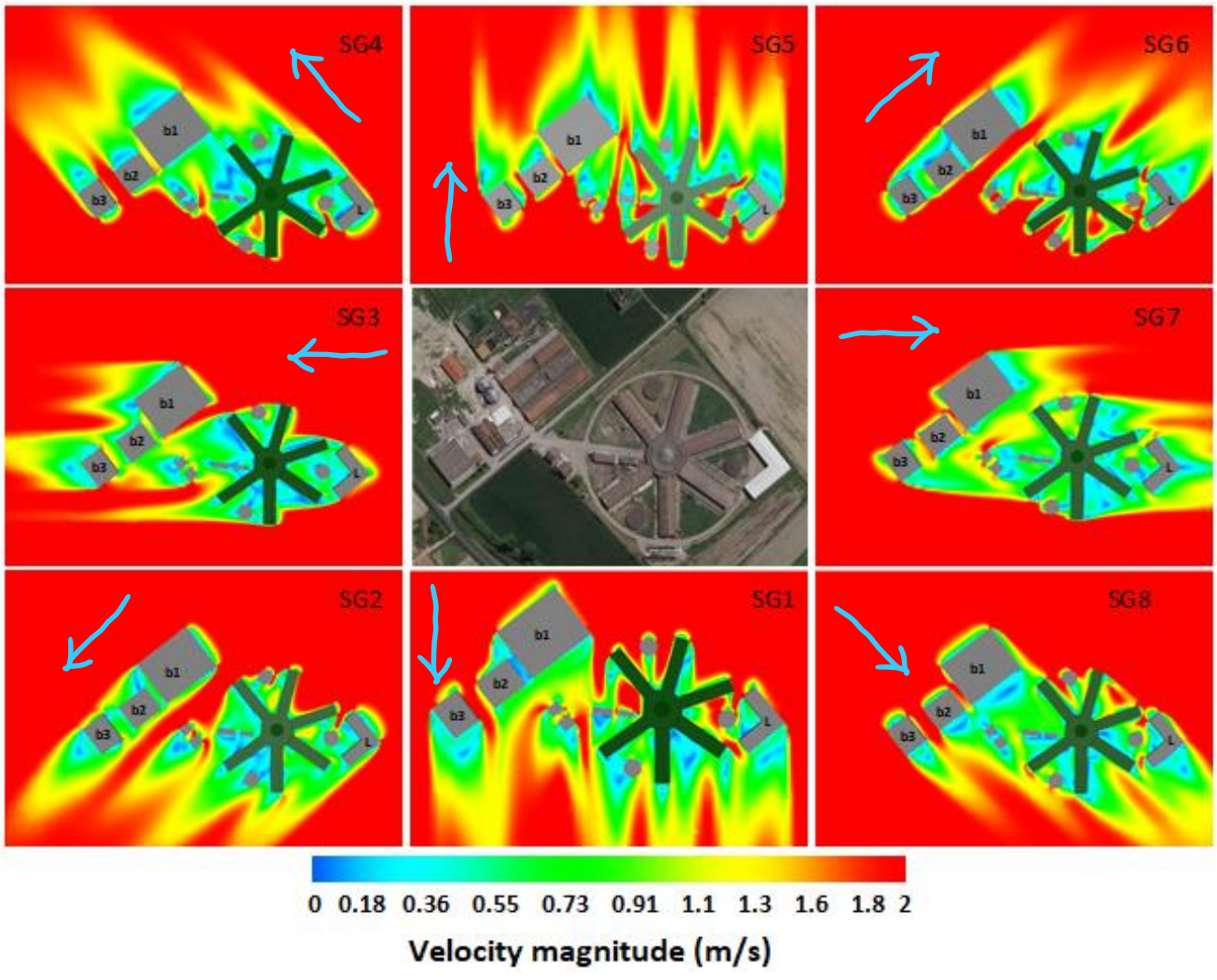

Figure 9. Outdoor velocity contours at 3.0 m from the g.l. for the scenarios from SG1 to SG8. The light blue arrows in the figure indicate the blowing direction of the wind.

Furtherly, in SG2 the possible negative effects related to the presence of the L-shaped building result limited, allowing an incoming air velocity about 1 m/s blowing towards the barn wings. The effect of the same building in case SG4 is slightly more evident, where it hinders the air flow between w3 and w4, creating low velocity areas, about 0.2 m/s close to the walls of the wings. As in the previous cases, the barn geometry affects w5 and w6 in SG2 and again w1 and w2 in SG4. SG6 is characterized by similar results to SG2, where the negative effects of the surrounding buildings are negligible and the ventilation of w2 and w3 is mainly affected by the barn geometry. In SG3 is significant for the wind magnitude and direction, the presence of the L building, which not only reduces the wind velocity on the wings w3 and w4 in close proximity, but also emphasizes the negative effects of the geometry. In fact, a reduced wind velocity characterized the whole structure, creating areas with low air velocity (lower 0.2 m/s) in the four wings (i.e., w1, w4, w5 and w6). Different results are verifiable in SG7 and SG8, because the three buildings b1, b2 and b3 play a significant role on the wind driven ventilation of the barn. In the SG7 case, all wings are affected by the presence of buildings b1, b2 and b3 approximately in the same way, with an air velocity reduction of about 40 %. The situation for w3, w4, and w5 is strengthened by the presence of the other wings, whose act as additional obstacles to the air flow. In the SG8 case, the negative effects are similar to SG7 for w1, w4, w5, and w6 whereas they are negligible for w2 and w3. These mutual interactions between wind action, wind direction, barn geometry and surrounding obstacles should be reflected in scenario-by-scenario ventilation efficiency reduction for some wings or, in other cases, for the whole pig barn.

3.2.2 Pressure coefficients and ventilation rate ratio

The CFD simulations on model A allow the calculation of the ventilation rate of the pig barn building as defined before. With reference to Eq. (11), the evaluation of the pressure coefficients C_{pw} and C_{pl}, for each scenario, have been obtained from the simulations for every wing of the pig barn, as a single building, and for the whole structure. The pressure coefficients have been considered at the middle height level of the windows, i.e., 3.0 m g.l. In Figure 10 (a), the trends of

the pressure coefficients for each wing, in the eight scenarios SG1-SG8, have been presented as values of (C_{pw} - C_{pl}), which show a high variability in relation to the wind direction. The wing w1 presents a value lower than 0.1 in case of wind blowing from South-East and North-West. Instead, w2 has the lowest pressure coefficients with wind from North, South and South-West. Similar results characterize w3 and w4, where the lowest value is related to wind from West.

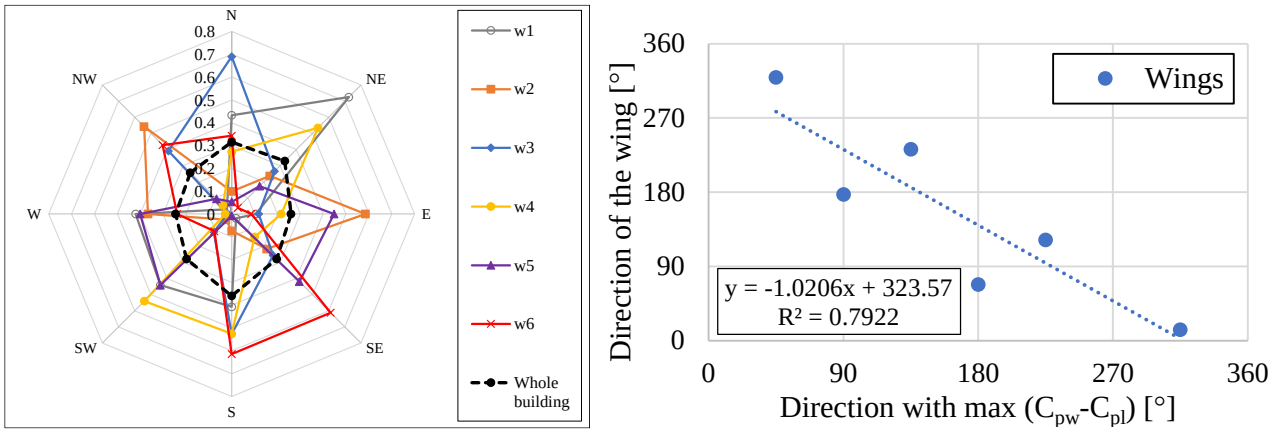

(a) (b)

Figure 10. Elaboration of the pressure coefficient results. (a) Values of (C_{pw}-C_{pl}) for each wing and for the whole pig barn for the 8 different wind directions analysed in the SG1-SG8 scenarios. (b) Relation of interpolation between the wing orientation and the wind direction responsible of the maximum value of pressure coefficient.

The wing w5 shows critical values in case of wind from North, South and North-West, while North-East and East are the smallest for w6 wing. The lowest value of pressure coefficient difference is 0.008 and is related to w5 in the SG5. In this case, the wing is parallel to the wind direction, which negatively affects the air flow pattern for the incoming air in w5. This could consist in a strong reduction of the ventilation of this wing. These outcomes confirm what has been observed in the velocity maps of Figure 9 since the ventilation in a wing depends not only on the surrounding buildings and on the whole building layout but also on the orientation of each single wing with respect to the orientation of the blowing wind. Furthermore, the possible relation between the orientation of a wing and the wind direction providing the maximum (C_{pw} - C_{pl}) value for that wing has been investigated. The results are shown in Figure 10 (b), assuming as wing direction, the orientation angle of the longitudinal axis with respect to North direction (e.g. North direction corresponds to the 0° direction). The six points related to the six wings are well aligned,

demonstrating that a correlation between the two quantities exists. In particular, the average difference between the optimal direction of the wind and the wing direction is equal to 101°, rather close to a right angle, confirming that despite the complex layout of the pig barn and the influence of the surrounding buildings, on average, each wing achieves its maximum ventilation efficiency when the wind blows along a direction orthogonal to the openings. This aspect could simplify the choice adopted in the management of the barn openings and also drive the possible retrofitting solutions for the building since each wing could be studied separately from the others since the indoor ventilation is mainly wind direction-driven. In order to obtain the overall ventilation efficiency, the $(C_{pw} - C_{pl})$ values have been calculated for the whole building and, having the wings same length, they have been calculated as the average value for the wings, as reported in Table 3. For the whole building, the values result more regular and they range from 0.24 (SG7 scenario) to 0.36 (SG5 scenario) for the different directions. Moreover, Table 3 shows the values of the $(C_{pw,ref} - C_{pl,ref})$ pressure coefficient difference calculated for the reference building previously defined (see Section 2.6.2). Moreover, the values of the ventilation rate ratio Q_R, for the eight SG scenarios, have been calculated based on Eq. (11) and Eq. (12). The Q_R values are reported in Table 3 and they range from 0.49 to 0.60. The lowest value has been detected in the case of wind blowing from West, while the highest value has been obtained for wind blowing from South.

Table 3

Values of the $(C_{pw} - C_{pl})$ pressure coefficient difference for each wing and for the whole pig barn. Values of the $(C_{pw,ref} - C_{pl,ref})$ pressure coefficient difference for the reference building and values of the relative ventilation rate ratio Q_R for each scenario SG.

Scenario (wind direction)	$(C_{pw} - C_{pl})$							$(C_{pw,ref} - C_{pl,ref})$ **Reference building**	Q_R
	w1	w2	w3	w4	w5	w6	Whole pig barns		
SG1(N)	0.433	0.099	0.690	0.273	0.053	0.343	0.315	1.011	0.56
SG2(NE)	0.725	0.236	0.265	0.534	0.173	0.038	0.329	1.011	0.57
SG3(E)	0.105	0.585	0.118	0.217	0.448	0.086	0.260	1.012	0.51
SG4(SE)	0.027	0.217	0.256	0.142	0.419	0.612	0.279	1.011	0.53
SG5(S)	0.407	0.074	0.527	0.525	0.008	0.614	0.359	1.011	0.60
SG6(SW)	0.441	0.035	0.111	0.540	0.441	0.107	0.279	1.011	0.53
SG7(W)	0.420	0.366	0.018	0.028	0.400	0.239	0.245	1.012	0.49
SG8(NW)	0.029	0.542	0.391	0.054	0.094	0.427	0.256	1.011	0.50

In general, by the ventilation rate ratio quantification, it is possible to conclude that the pig barn is characterized by a ventilation rate about 50% of the ventilation rate of the reference building, having the best ventilation conditions.

3.2.3 Assessment of surrounding buildings and geometry effects

The ventilation rate ratio should be useful to quantify the ventilation rate reduction caused by several aspects, such as building geometry, layout and in-elevation conformation, building orientation, or surrounding bodies influence. In the case study, the ventilation rate ratios show a considerable reduction of the potential ventilation rates, calculated with respect to the reference building, and rather homogeneous for the different wind directions. In fact, the highest ventilation rate ratio, i.e., 0.60 (60%), is related to the SG5 scenario with wind blowing from South direction. In this scenario, the buildings around the barn don't influence in an important way the wind flow, which can reach the pig barn without any obstacles. On the other hand, the smallest ventilation rate ratio is equal to 0.49 (49%) in the SG7 scenario. In this case, the final ventilation rate is the sum of the effects from wing interactions and interference with surrounding buildings, but as can be noted, the presence of other buildings plays a marginal role, able to worsen the whole ventilation rate ratio of 11%. So, for the case study investigated, another important consideration inducing a possible simplification is that probably in the CFD model the surrounding buildings could be omitted since they play, as a whole, a marginal role.

3.3 Seasonal effects evaluation

Starting from the preliminary aspects discussed above, the natural ventilation efficiency could be significantly different during the year for the various wings of the barn. In the following, starting from the analysis of the internal air flow distribution conducted for two different seasons, i.e., warm and cold, an evaluation of the representative conditions of the barn, in terms of ventilation rate, is achieved with the main aim to provide a useful indication for the ventilation management of the single wing.

3.3.1 Velocity patterns

For the evaluation of the seasonal effects, 7 different scenarios have been considered: 4 scenarios for the warm season, i.e. SS1, SS2, SS3 and SS4, and 3 scenarios for cold season, i.e. SS5, SS6 and SS7. The direction of the blowing wind, i.e. the boundary condition considered in the CFD simulation, for each scenario, is reported in Table 2 and is represented by the black arrows in Figure 11 and Figure 13. For the definition of the wind profile the average velocity values at 10m g.l. reported in Table 2 have been used.

The results obtained from the model A, before discussed, suggest that based on different wind direction and magnitude the wings can be differently ventilated. This aspect has been observed also in the results of the model B, under the 7 scenarios investigated (SS1-SS7), the 4 scenarios for the warm season and 3 scenarios for cold season (see Table 2). As far as the warm season is concerned, the contour maps of the velocity magnitude and distribution at 0.5 m from the pavement level are shown in Figure 11. This level has been selected because it is the most representative level for investigate the conditions of the pigs inside the pens. In these scenarios, the wind magnitude ranges from about 1.4 to 2.0 m/s. For example, in SS1, the air velocity magnitude in the six wings is under 0.18 m/s in most of the pen areas. Few areas characterized by higher velocity (> 0.27 m/s) can be observed in w1, w6 and marginally, close to the lateral windows in w4. Moreover, w4 and w3 wings are characterized by a small area of very low air velocity (about 0.09 m/s) in the pens closer to the center building.

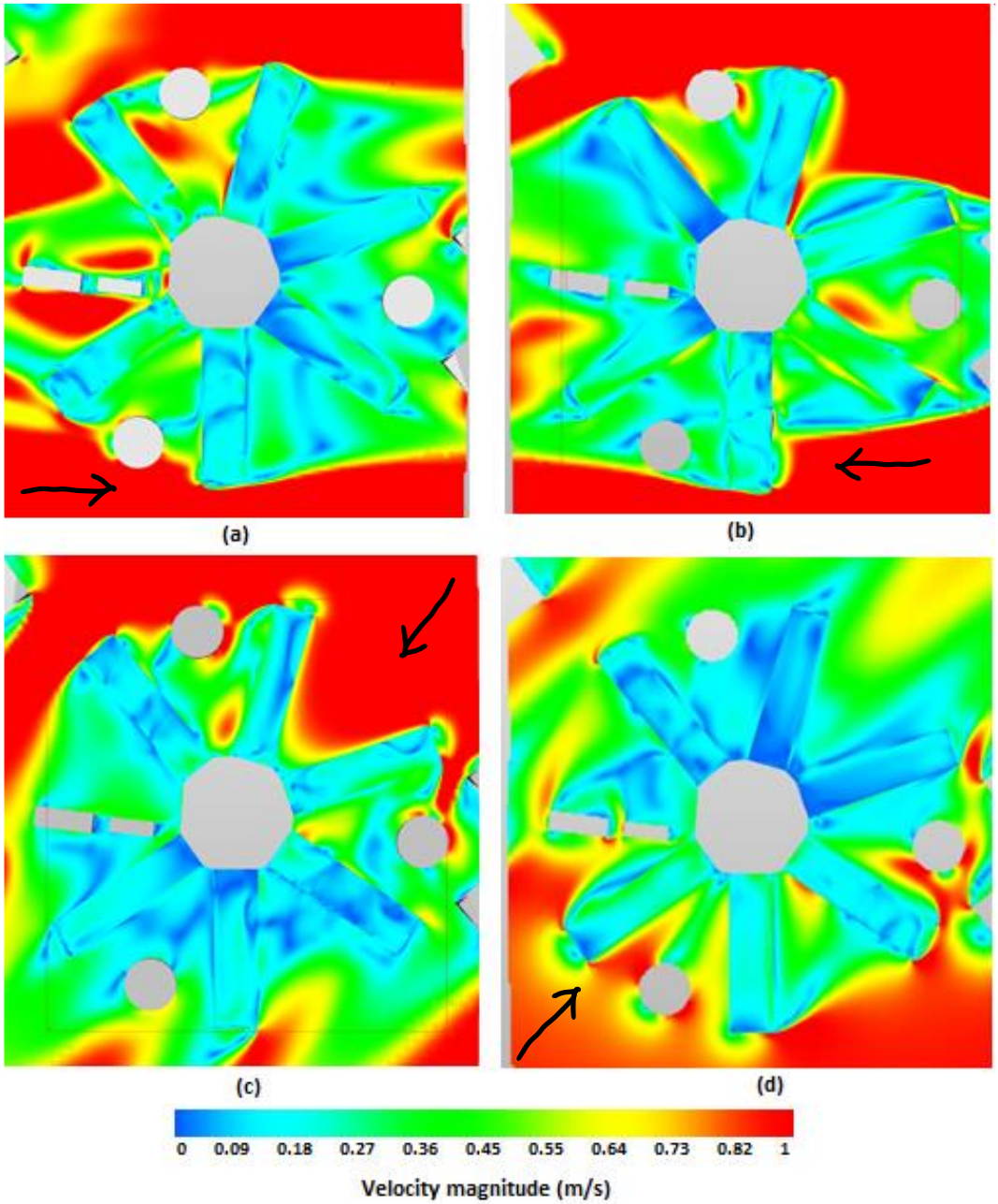

Figure 11. Velocity contours at 0.50 m from the inner pavement level for the different scenarios of the warm season: (a) SS1, (b) SS2, (c) SS3 and (d) SS4. The black arrows in the figure indicate the blowing direction of the wind.

These results confirm the previous outcomes observed in the SG7 scenario, where all wings are negatively affected by the sum of the effects coming from the presence of surrounding bodies and the layout of the building. Similar results are visible for scenario SS3 in Figure 11 (c). The air velocity distribution and magnitude are analogues in the whole barn with a few areas characterized by the highest velocity (i.e. $v \geq 0.27$ m/s) in w1, w2 and w3. Instead, different ventilation conditions

between the different wings can be found in the other three scenarios SS2, SS3 and SS4. In Figure 11 (b), almost the entire wing w4 presents an air velocity higher than 0.27 m/s. Nevertheless, the L-building at SE of the barn, reduces the indoor velocity in the pens at the extremity of the wing. In this scenario, w1 is in the worst condition with air velocity ≤ 0.18 m/s and a significant percentage of the pens have very low velocity, i.e., $v \leq 0.09$ m/s. Similar conditions characterize the scenario SS4, showed in Figure 11 (d), where the wings w5 and w6 are characterized by a higher air velocity magnitude if compared to the others, due to their orientation and absence of obstacles. In this case, both wings w2 and w3 have indoor air velocity ≤ 0.18 m/s for their whole area with numerous pens even at a velocity $v \leq 0.09$ m/s. However, in the three cases of the cold season, generally the air velocity magnitude and distribution are slightly improved when compared to the similar cases of the warm season. Overall, during the warm and cold seasons, w1, w2, and w3 wings suffer more than the others in terms of ventilation. On the other hand, w5 and w4 wings present in the cases analysed, ventilation conditions slightly better even if they do not seem optimal for pigs fattening. A quantitative analysis and the comparison between the indoor air velocity in each wing have been conducted, based on the air velocity obtained by means of the CFD simulations at a level 0.5 m. In particular, the approach envisages the definition of 14 equally spaced (spacing of 1 m) profiles in the plan under analysis, as presented in Figure 13.

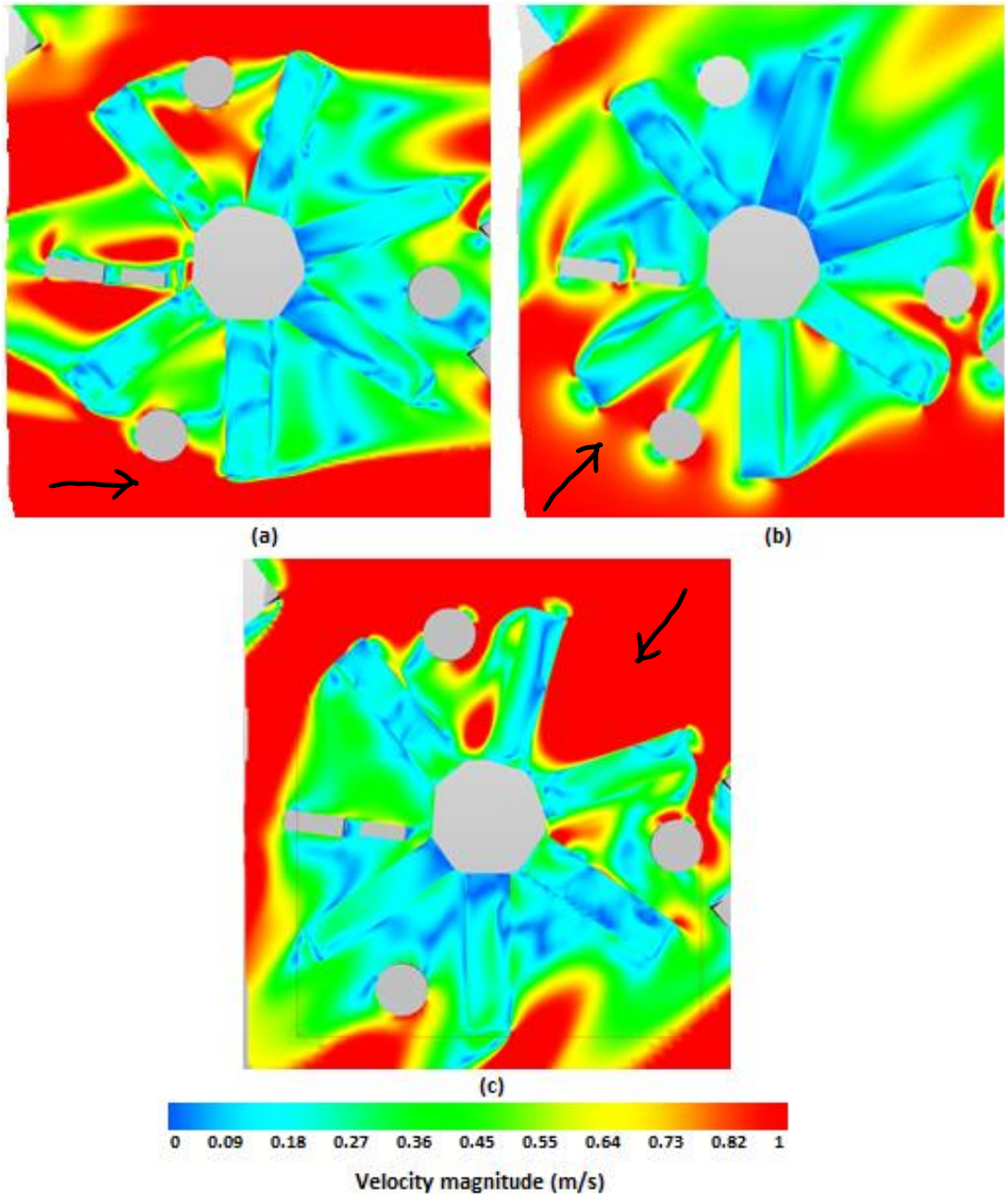

Figure 12. Velocity contours at 0.50 m from the inner pavement level for the different scenarios of the cold season: (a) SS5, (b) SS6 and (c) SS7. The black arrows in the figure indicate the blowing direction of the wind.

This procedure has been performed for each wing, for the seven scenarios SS1-SS7. In this way, not only the average indoor air velocity, representative of the condition of the two lanes of pens, has been defined, but even the average velocity for both the seasons can be determined.

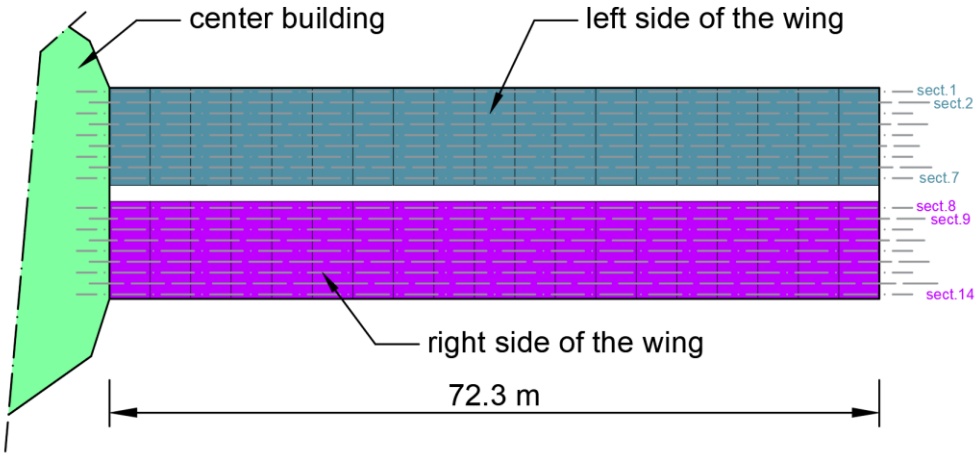

Figure 13. Position of the 14 longitudinal sections used for the calculation of the average velocity of the pens on the right side and on the left side of a wing.

As a representative example, the distribution of the indoor air velocity obtained for the w5 wing in scenario SS2, is exhibited in Figure 14 (a). The figure shows the higher velocities along one perimeter longitudinal wall of the wing and progressively decreasing moving to the opposite longitudinal wall. This is rather typical in buildings in presence of cross-ventilation mechanism. In Figure 14 (b), the velocity trends (average and average ± standard deviation) in the pens on the right side and on the left side, with respect to the central corridor of the wing, have been obtained starting from the data of the 14 longitudinal sections.

Then, the average velocity of the warm and cold seasons, respectively, has been calculated with this methodology for the different wings and have been collected in Table 4 and Table 5. As Table 4 shows, velocity is significantly different between the two sides, i.e., right and left, of each wing practically in all scenarios except for: wing 2 in SS2, wing 4 in SS3 and wing 5 in SS1. In SS1, w1 and w6 are characterized by high and homogenous air velocity in all pens, such as w3, w4, w5 and w6 in SS2. The last three maintain this condition in SS4, while instead, w3 is the only one showing this situation in SS3. By considering the whole warm season, the average values from the two sides show less pronounced differences. The main variations in the season interest the w2 and w4 wings where the air velocities at the right side respectively, are 25% and 20% lower than the left side.

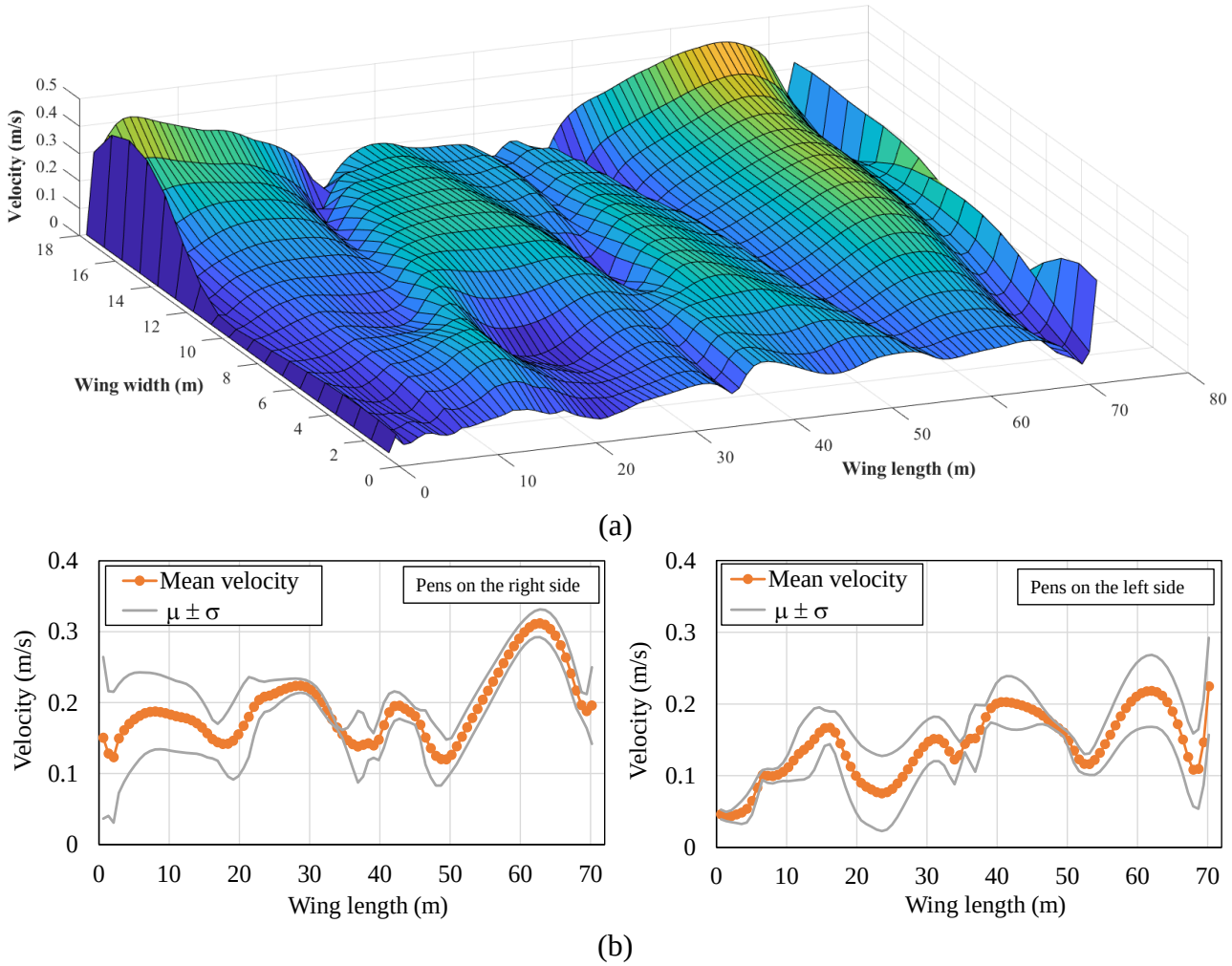

Figure 14. Elaboration of the velocity magnitude. (a) Example of velocity magnitude of the wing w5 for scenario SS2 at 0.50 m from the pavement level. (b) Velocity trends in the pens on the right side and on the left side with respect to the corridor of the wing.

Table 4

Velocity magnitude at 0.5 m g.l. for the various wings and for the different scenarios of the warm season.

	Right side velocity (m/s)					Left side velocity (m/s)				
Wing	SS1 (W)	SS2 (E)	SS3 (NE)	SS4 (SW)	Average for the season	SS1 (W)	SS2 (E)	SS3 (NE)	SS4 (SW)	Average for the season
w1	0.240	0.071	0.123	0.134	0.144	0.181	0.117	0.129	0.091	0.134
w2	0.132	0.115	0.093	0.057	0.105	0.126	0.135	0.216	0.057	0.139
w3	0.105	0.146	0.256	0.058	0.146	0.140	0.175	0.171	0.095	0.150
w4	0.064	0.306	0.099	0.150	0.157	0.225	0.257	0.100	0.144	0.190
w5	0.149	0.192	0.136	0.178	0.163	0.146	0.140	0.116	0.224	0.150
w6	0.159	0.201	0.170	0.271	0.193	0.272	0.232	0.107	0.211	0.209

For all the sides, on average, w4, w5, and w6 have the higher indoor air velocity magnitude. As far as the cold season in Table 5 is concerned, the wings show similar velocity magnitude in the whole period.

Table 5

Velocity magnitude at 0.5 m g.l. for the various wings and for the different scenarios of the cold season.

Wing	Right side velocity (m/s)				Left side velocity (m/s)			
	SS5 (W)	SS6 (SW)	SS7 (NE)	Average for the season	SS5 (W)	SS6 (SW)	SS7 (NE)	Average for the season
w1	0.264	0.144	0.160	0.210	0.201	0.098	0.169	0.164
w2	0.148	0.060	0.123	0.117	0.144	0.062	0.282	0.144
w3	0.123	0.063	0.333	0.142	0.148	0.102	0.227	0.148
w4	0.070	0.155	0.130	0.106	0.246	0.155	0.131	0.198
w5	0.166	0.190	0.175	0.175	0.158	0.240	0.151	0.181
w6	0.292	0.226	0.136	0.244	0.176	0.291	0.225	0.219

From the contour maps, SS5 should present similarities to SS1, SS6 to SS4 and SS7 to SS3. However, in the cold season, in SS5, not only w1 and w6 but also w2, w3 and w5 are characterized by high and homogeneous air velocity in both right and left sides. Moreover, results of the SS6 confirm those observed in the warm season. Instead, in SS7 all the six wings show high and homogeneous air velocity in both sides differently from the warm season. Again, on the basis of the entire cold season, the average results show moderate differences between the different wings and the different sides. The main variations interest w1, where the air velocity at the left side is 22% lower than the velocity in the right side, and w4 where the air velocity at the right side are 47% lower than the left side. Despite this, w5 and w6 are characterized by the higher air velocity magnitude as for the warm season, as also w1 and w3.

Furthermore, for the warm season, the average velocity in the various wings (see Table 4) ranges from 0.10 m/s to 0.22 m/s for the pens in the right side whereas it ranges from 0.13 m/s to 0.21 m/s in the left side pens. These values are very low if compared to the optimal values expected in a pig barn during warm season when the animals can suffer serious heat stress effects due to high temperature (Vitali et al. 2021a). The average velocity has similar range in the cold season (see Table 5). In fact, the average velocity in the various wings ranges from 0.10 m/s to 0.24 m/s for the pens in the right side whereas it ranges from 0.14 m/s to 0.22 m/s in the lift side pens. The depicted scenario entails suitable retrofitting interventions in order to guarantee animal welfare, especially in the warm season.

3.3.2 Expected seasonal ventilation rate

Most of the parameters characterizing the suitability of the indoor environmental conditions, strongly depend on the ventilation rate of the wings of the building. In particular, in the case study investigated here, the ventilation rates of the pig barn have been assessed for both warm and cold seasons, based on the wind velocity, at a level of 3.0m (mid-height of the wall openings), obtained for the various scenarios by the statistical analysis and the pressure coefficient values obtained in the previous sections (see Table 2). In particular, the pressure coefficient differences have been calculated as the weighted average of the results obtained in SG2, SG3, SG6 and SG8 in the warm season and in SG2, SG6 and SG8 in the cold season. The weights assumed for combining the various scenarios have been the percentage of hours characterizing the presence of each scenario with respect to the total number of hours of the entire investigated period. The ventilation rates have been calculated by means of the Eq.(11) for all wings and the main results are reported in Table 6. It is worth to note that the values of Q have been also computed, for the various cases, by integrating the normal velocity vectors over the opening surfaces. The value of the maximum difference between Q values provided by Eq. (11) and those obtained by integration is about 7%. The average difference is about 4% and it confirms the reliability of the study.

Table 6

Ventilation rate Q of the six wings of the pig barn, for warm and cold seasons.

	Q in m^3/s (m^3/h)	
Wing	Warm season	Cold season
w1	81 080	102 379
w2	78 027	71 561
w3	43 187	37 975
w4	64 149	60 925
w5	81 518	88 089
w6	45 826	57 952

By assuming that each wing could house at the maximum 1064 pigs (i.e. 28 pigs/pen × 38 pens/wing), and considering as minimum need a ventilation rate per animal about 20 m^3/h and 115 m^3/h for the cold and warm seasons respectively (RER Regione Emilia Romagna 2013), it suggests that during the cold season all wings have a suitable ventilation (the minimum requested ventilation

rate for a wing is about 21 280 m^3/h). On the other hand, during the warm season when the minimum requested ventilation rate for a wing is about 122 360 m^3/h, w1, w2 and w5 reach about 70% of the minimum suggested, while the other wings could experience conditions abundantly non-suitable in terms of ventilation rate. This event can be avoided, of course, by reducing the number of animals per wing or by designing suitable retrofitting interventions, e.g. introducing ventilation systems, in some wings of the pig barn.

3.3.3 Assessment of the seasonal effects

The warm and cold seasons are respectively characterized by four and three prevailing wind directions, covering 65% of the hours of the season period. In both the seasons the wind directions repeated, West, North-East, and South-West, marginally varying in terms of reference wind velocity (measured at 10.0m from g.l.). From the results of the simulations, it appears that in both the periods the wing w3 has the lowest ventilation rate. This situation reflects the sum of the negative effects of the interaction with the surrounding buildings and the layout of the pig barn and explains the presence of low indoor air velocities. The ventilation rates of the wings w1, w2, and w5 confirm the suitable conditions of the natural ventilation of the wings. W1 and w2, contrary to what has been highlighted by the contour maps, have values of ventilation rate almost acceptable in both seasons, even if the indoor velocity inhomogeneity from the right side to the left side of the pen area, can be considerable. This aspect seems to be attributable to the geometrical orientation of the wing and also to indoor turbulence and mixing mechanisms due to the considerable size of the building. Finally, the wing w6 demonstrates high indoor velocities in the qualitative and quantitative analysis in all seasons, but on the other hand presents insufficient ventilation rate during the warm period. All these aspects asked for the planning of different retrofitting interventions for the various wings of the existing pig barn.

The results of the paper, although derived for a case study with a particular layout, pave a way that can be applied to a large livestock building stock characterized by the need of suitable ventilation rates all along the time. In fact, the possibility to precisely evaluate, with CFD simulations, the air

velocity inside the buildings could provide indication about both the most critical periods of the year and the pens of the barn less comfortable for the animals. These outcomes can be used for two main purposes. The first involves the management of the herd because the farmer can take advantage of these results for planning in a more efficient way the whole fattening process (for instance by modifying the number of animals per pen or using the different portions of the barn for different fattening stage in order to minimize the negative impact of the indoor conditions on the animals). The second concerns on one hand the selection of the most effective retrofitting interventions on the existing structures and on the other hand can drive the design of more efficient new livestock buildings. For example, for the most characteristic wind directions at the site, the most efficient open/close configuration of roof and lateral openings can be established and used for the management of the windows of the different portions of the livestock housing.

Finally, it seems useful to remark again that, even if the method adopted in the paper is rigorous from a scientific point of view, CFD simulations have been realized on numerical models considering some simplifications. For instance, the analysed pens had no animals inside. Moreover, the temperature and relative humidity, specific for each simulation, have been assumed constant in the whole domain and then, the possible buoyancy effects have been not considered. The introduction of the animal presence and their interaction with the indoor climate will be investigated in future work after the definition of the evapotranspiration model simulating the biology of the animals.

Furthermore, despite the complex layout of the pig barn each wing achieves its maximum ventilation efficiency when the wind blows along to the direction perpendicular to the openings. This result can be useful for other and future work, also applied to other buildings, since it shows that, for a preliminary assessment of the indoor ventilation conditions, each wing could be studied separately from the others. In addition, the performance indicator named *Ventilation rate ratio* defined in this paper, has been proposed for a preliminary quantification of the reduction of the ventilation efficiency of a building with complicated geometry compared to that of a simple

equivalent building considered as reference. The *Ventilation rate ratio* can be calculated, theoretically, for every building layout and then it represents a further outcome of the paper which is transferable to several other buildings.

4. Conclusions

This paper presents the main results of the CFD simulations solved on an existing pig barn characterized by a complex shape. The results obtained allow to understand the behaviour of the livestock structure in terms of ventilation conditions with a general validity, independently from specific window opening conditions depending on daily management choices or any mechanical ventilation equipment. The study has focused on the building ventilation performances and how they are affected by the complex building geometry. The numerical modelling has allowed a parametric analysis for eight wind directions, has provided information on the external flow patterns and the evaluation of effects on the internal mixing. The main outcomes of the paper are:

- the combination of the presence of surrounding buildings close to the barn and the layout of the pig barn itself determines a significant reduction of the pressure coefficient differences measured on opposite walls; the reductions range from 40% to 50% with respect to the values obtained for the reference building described in the paper.
- the indoor air flow distribution, based on the average air velocity in the pens, showed very different conditions for the two sides of the pens, in several wings, for both investigated seasons;
- during the cold season all wings have suitable ventilation, presenting ventilation rates higher than the minimum requested. On the other hand, during the warm season, three wings only reach the 70% of the minimum suggested, while the other three seems characterized by conditions even worse;
- despite the complex layout of the pig barn and the influence of the surrounding buildings, each wing achieves its maximum ventilation efficiency when the wind blows along to the direction perpendicular to the openings. This could simplify the management choices of the

barn openings and also drive the possible retrofitting solutions for the building since each wing could be studied separately from the others;

- the proposal of a dimensionless parameter Q_R, called ventilation rate ratio, measuring the effects of the building geometry on the ventilation efficiency calculated with respect to a reference building;

Results on the indoor airflow, in naturally ventilated livestock buildings, are fundamental to check animal welfare and guarantee efficient and sustainable production. On the other hand, the control of gaseous emissions and the monitoring of environmental conditions in the areas surrounding livestock buildings are fundamental actions, especially in those territories with high concentration of intensive animal farms. With regard to these aspects, knowledge of the outdoor airflow are fundamental to assess the gas concentrations and investigate the gases dispersion in the areas around a livestock building since air velocity and airflow are driving factors for the livestock emissions like, for instance, methane, ammonia and carbon dioxide. Moreover, the outcomes of the paper provide useful indications for the management of the livestock structure since they could be used for the choice of the most favourable barn pens for the different finishing pig groups characterized by different ages and fattening stages but also for the suitable planning of possible ventilation retrofitting interventions.

Acknowledgements

The authors would like to thank the Project “Progetto Filiera F61 – Reg. (UE) 1305/2013 – PSR 2014/2020 DGR Emilia-Romagna n. 227/2017 e s.m.i. - FOCUS AREA 3A - Operazione 16.2.01 capofila “Fontane del Duca s.r.l” and in particular Prof. Paolo Trevisi, Scientific Responsible of the University of Bologna’s research team, for providing the case-study farm on which the authors have carried out the study. The authors would also like to thank the Farm “Stalla Tullie” (Rolo, Italy), for the kind availability during the surveys.

References

Autodesk. 2020. “Inventor.” 2020. https://www.autodesk.it/products/inventor%0A.

Bjerg, B., K. Svidt, G. Zhang, and S. Morsing. 2000. “The Effects of Pen Partitions and Thermal Pig Simulators on Airflow in a Livestock Test Room.” *Journal of Agricultural and Engineering Research* 77 (3): 317–26. https://doi.org/10.1006/jaer.2000.0596.

CEN. 2010. *EN 1991-1-4:2005 Eurocode 1: Actions on Structures - Part 1-4: General Actions - Wind Actions*. Edited by European Commitee for Standardization. Brussels.

Chantziaras, Ilias, Dimitri De Meyer, Lode Vrielinck, Tommy Van Limbergen, Carlos Pineiro, Jeroen Dewulf, Ilias Kyriazakis, and Dominiek Maes. 2020. “Environment-, Health-, Performance- and Welfare-Related Parameters in Pig Barns with Natural and Mechanical Ventilation.” *Preventive Veterinary Medicine* 183 (September): 105150. https://doi.org/10.1016/j.prevetmed.2020.105150.

Choi, Hong Lim, Sang Hwa Han, Louis D. Albright, and Won Kyung Chang. 2011. “The Correlation between Thermal and Noxious Gas Environments, Pig Productivity and Behavioral Responses of Growing Pigs.” *International Journal of Environmental Research and Public Health* 8 (9): 3514–27. https://doi.org/10.3390/ijerph8093514.

Chu, Chia Ren, and Ting Wei Lan. 2019. “Effectiveness of Ridge Vent to Wind-Driven Natural Ventilation in Monoslope Multi-Span Greenhouses.” *Biosystems Engineering* 186: 279–92. https://doi.org/10.1016/j.biosystemseng.2019.08.006.

Chu, Chia Ren, Ting Wei Lan, Ren Kai Tasi, Tso Ren Wu, and Chih Kai Yang. 2017. “Wind-Driven Natural Ventilation of Greenhouses with Vegetation.” *Biosystems Engineering* 164 (December): 221–34. https://doi.org/10.1016/J.BIOSYSTEMSENG.2017.10.008.

CIBSE. 2015. *CIBSE Guide A: Environmental Design*. United Kingdom: The Chartered Institution of Building Services Engineers (CIBSE).

CNR. 2019. *CNR-DT 207 R1/2018 “Istruzioni per La Valutazione Delle Azioni e Degli Effetti Del Vento Sulle Costruzioni.”* Consiglio. Roma.

Costola, D, B Blocken, and J L M Hensen. 2009. “Overview of Pressure Coefficient Data in Building Energy Simulation and Airflow Network Programs.” *Building and Environment* 44 (10): 2027–36. https://doi.org/10.1016/j.buildenv.2009.02.006.

CSPFea. 2020. “VENTO Software.” 2020. http://vento-cfd.com.

Emilia Romagna region. 2020. “Arpae.” 2020. https://www.arpae.it/.

Espinoza, Karlos, Alejandro López, Diego L. Valera, Francisco D. Molina-Aiz, José A. Torres, and Araceli Peña. 2017. “Effects of Ventilator Configuration on the Flow Pattern of a Naturally-Ventilated Three-Span Mediterranean Greenhouse.” *Biosystems Engineering* 164: 13–30. https://doi.org/10.1016/j.biosystemseng.2017.10.001.

Golubić, Dino, Walter Meile, Günter Brenn, and Hrvoje Kozmar. 2020. “Wind-Tunnel Analysis of Natural Ventilation in a Generic Building in Sheltered and Unsheltered Conditions: Impact of Reynolds Number and Wind Direction.” *Journal of Wind Engineering and Industrial Aerodynamics* 207 (June 2019). https://doi.org/10.1016/j.jweia.2020.104388.

Gonçalves de Oliveira, Débora Caroline, Melissa Selaysim Di Campos, Nady Passé-Coutrin, Cristel Onésippe Potiron, Ketty Bilba, Marie Ange Arsène, and Holmer Savastano Junior. 2021. “Modeling of the Thermal Performance of Piglet House with Non-Conventional Floor System.” *Journal of Building Engineering* 35 (December 2019). https://doi.org/10.1016/j.jobe.2020.102071.

Halsey, Troy. 2010. “Chapter 14 - Environment Design.” In *Freelancer’s Guide to Corporate Event Design*, edited by Troy Halsey, 239–54. Boston: Focal Press. https://doi.org/https://doi.org/10.1016/B978-0-240-81224-3.00016-9.

Huang, Wei-Xi, and Fang-Bao Tian. 2019. “Recent Trends and Progress in the Immersed Boundary Method.” *Proceedings of the Institution of Mechanical Engineers, Part C: Journal of Mechanical Engineering Science* 233 (23–24): 7617–36. https://doi.org/10.1177/0954406219842606.

Iqbal, Ahsan, Alireza Afshari, Hans Wigö, and Per Heiselberg. 2015. “Discharge Coefficient of Centre-Pivot Roof Windows.” *Building and Environment* 92: 635–43. https://doi.org/https://doi.org/10.1016/j.buildenv.2015.05.034.

Jackson, Paul, Abozar Nasirahmadi, Jonathan H. Guy, Steve Bull, Peter J. Avery, Sandra A. Edwards, and Barbara Sturm. 2020. “Using CFD Modelling to Relate Pig Lying Locations to Environmental Variability in Finishing Pens.” *Sustainability (Switzerland)* 12 (5). https://doi.org/10.3390/su12051928.

Ji, Y, M J Cook, V Hanby, D G Infield, D L Loveday, and L Mei. 2008. “CFD Modelling of Naturally Ventilated Double-Skin Facades with Venetian Blinds.” *Journal of Building Performance Simulation* 1 (3): 185–96. https://doi.org/10.1080/19401490802478303.

Karava, P., T. Stathopoulos, A. K. Athienitis, Dino Golubić, Walter Meile, Günter Brenn, and Hrvoje Kozmar. 2011. “Airflow Assessment in Cross-Ventilated Buildings with Operable Façade Elements.” *Journal of Wind Engineering and Industrial Aerodynamics* 46 (June 2019): 266–79. https://doi.org/10.1016/j.buildenv.2010.07.022.

Kim, Rack woo, Se woon Hong, In bok Lee, and Kyeong seok Kwon. 2017. “Evaluation of Wind Pressure Acting on Multi-Span Greenhouses Using CFD Technique, Part 2: Application of the CFD Model.” *Biosystems Engineering* 164: 257–80. https://doi.org/10.1016/j.biosystemseng.2017.09.011.

King, Marco Felipe, Hannah L. Gough, Christos Halios, Janet F. Barlow, Adam Robertson, Roger Hoxey, and Catherine J. Noakes. 2017. “Investigating the Influence of Neighbouring Structures on Natural Ventilation Potential of a Full-Scale Cubical Building Using Time-Dependent CFD.” *Journal of Wind Engineering and Industrial Aerodynamics* 169 (August):

265–79. https://doi.org/10.1016/j.jweia.2017.07.020.

Launder, B.E., and D.B. Spalding. 1983. “The Numerical Computation of Turbulent Flows.” In *Numerical Prediction of Flow, Heat Transfer, Turbulence and Combustion*, 96–116. Elsevier. https://doi.org/10.1016/b978-0-08-030937-8.50016-7.

Liu, Wei, Mingang Jin, Chun Chen, and Qingyan Chen. 2016. “Optimization of Air Supply Location, Size, and Parameters in Enclosed Environments Using a Computational Fluid Dynamics-Based Adjoint Method.” *Journal of Building Performance Simulation* 9 (2): 149–61. https://doi.org/10.1080/19401493.2015.1006525.

Liu, Xiaodong, Li Yang, and Shengnan Niu. 2021. “Research on the Effect of Different Position on Classroom Ventilation in a ‘L’ Type Teaching Building.” *Journal of Building Engineering* 33 (September 2020): 101852. https://doi.org/10.1016/j.jobe.2020.101852.

Liu, Xiaoping, Jianlei Niu, Marco Perino, and Per Heiselberg. 2008. “Numerical Simulation of Inter-Flat Air Cross-Contamination under the Condition of Single-Sided Natural Ventilation.” *Journal of Building Performance Simulation* 1 (2): 133–47. https://doi.org/10.1080/19401490802250462.

Meng, Fan Qin, Bao Jie He, Jin Zhu, Dong Xue Zhao, Amos Darko, and Zi Qi Zhao. 2018. “Sensitivity Analysis of Wind Pressure Coefficients on CAARC Standard Tall Buildings in CFD Simulations.” *Journal of Building Engineering* 16 (January): 146–58. https://doi.org/10.1016/j.jobe.2018.01.004.

Mossad, R. R. 2009. “Optimization of the Ventilation System for a Forced Ventilation Piggery.” *Journal of Green Building* 4 (4): 112–32. https://doi.org/10.3992/jgb.4.4.113.

Ramirez, N, Afshin Afshari, and L Norford. 2018. “Validation of Simplified Urban-Canopy Aerodynamic Parametrizations Using a Numerical Simulation of an Actual Downtown Area.” *Boundary-Layer Meteorology* 168 (1): 155–87. https://doi.org/10.1007/s10546-018-0345-7.

RER Regione Emilia Romagna. 2013. “Tecnologie per l’allevamento Dei Suini.” *I Supplementi Di Agricoltura*, 2013.

Richards, P J, and R P Hoxey. 1993. “Appropriate Boundary Conditions for Computational Wind Engineering Models Using the K-ϵ Turbulence Model.” *Journal of Wind Engineering and Industrial Aerodynamics* 46–47: 145–53. https://doi.org/https://doi.org/10.1016/0167-6105(93)90124-7.

Rong, Li, Peter V. Nielsen, Bjarne Bjerg, and Guoqiang Zhang. 2016. “Summary of Best Guidelines and Validation of CFD Modeling in Livestock Buildings to Ensure Prediction Quality.” *Computers and Electronics in Agriculture* 121: 180–90. https://doi.org/10.1016/j.compag.2015.12.005.

Saha, Chayan Kumer, Qianying Yi, David Janke, Sabrina Hempel, Barbara Amon, and Thomas Amon. 2020. “Opening Size Effects on Airflow Pattern and Airflow Rate of a Naturally Ventilated Dairy Building-A CFD Study.” *Applied Sciences (Switzerland)* 10 (17). https://doi.org/10.3390/app10176054.

Swami, MV, and Subrato Chandra. 1987. “Procedures for Calculating Natural Ventilation Airflow Rates in Buildings.” *ASHRAE Final Report FSEC-CR-163-86*, 130.

Teitel, Meir, and Erez Wenger. 2014. “Air Exchange and Ventilation Efficiencies of a Monospan Greenhouse with One Inflow and One Outflow through Longitudinal Side Openings.”

Biosystems Engineering 119: 98–107. https://doi.org/10.1016/j.biosystemseng.2013.11.001.

Tomasello, N., F. Valenti, G. Cascone, and S.M.C. Porto. 2019. "Development of a CFD Model to Simulate Natural Ventilation in a Semi-Open Free-Stall Barn for Dairy Cows." *Buildings* 9 (8). https://doi.org/10.3390/buildings9080183.

Tominaga, Y, A Mochida, R Yoshie, H Kataoka, T Nozu, Masaru Yoshikawa, and T Shirasawa. 2008. "AIJ Guidelines for Practical Applications of CFD to Pedestrian Wind Environment around Buildings." *Journal of Wind Engineering and Industrial Aerodynamics* 96: 1749–61.

Troy Halsey. 2010. *The Freelancer's Guide to Corporate Event Design: From Technology Fundamentals to Scenic and Environmental Design*. New York: Routledge. https://doi.org/https://doi.org/10.4324/9780080960920.

Tu, Jiyuan, Guan-Heng Yeoh, and Chaoqun Liu. 2018. "Some Advanced Topics in CFD." In , edited by Jiyuan Tu, Guan-Heng Yeoh, and Chaoqun B T - Computational Fluid Dynamics (Third Edition) Liu, 369–417. Butterworth-Heinemann. https://doi.org/https://doi.org/10.1016/B978-0-08-101127-0.00009-X.

Vitali, Marika, Elena Santacroce, Federico Correa, Chiara Salvarani, Francesca Paola Maramotti, Barbara Padalino, and Paolo Trevisi. 2020. "On-Farm Welfare Assessment Protocol for Suckling Piglets: A Pilot Study." *Animals* 10 (6): 1–21. https://doi.org/10.3390/ani10061016.

Vitali, Marika, Enrica Santolini, Marco Bovo, Patrizia Tassinari, Daniele Torreggiani, and Paolo Trevisi. 2021a. "Behavior and Welfare of Undocked Heavy Pigs Raised in Buildings with Different Ventilation Systems." https://doi.org/10.3390/ani11082338.

———. 2021b. "Behavior and Welfare of Undocked Heavy Pigs Raised in Buildings with Different Ventilation Systems." *Animals 2021, Vol. 11, Page 2338* 11 (8): 2338. https://doi.org/10.3390/ANI11082338.

Wang, K., Q. Pan, and K. Li. 2017. "Computational Fluid Dynamics Simulation of the Hygrothermal Conditions in a Weaner House in Eastern China." *Transactions of the ASABE* 60 (1): 195–205. https://doi.org/10.13031/trans.11655.

Wang, Xiaoshuai, Guoqiang Zhang, and Christopher Y. Choi. 2018. "Effect of Airflow Speed and Direction on Convective Heat Transfer of Standing and Reclining Cows." *Biosystems Engineering* 167: 87–98. https://doi.org/10.1016/j.biosystemseng.2017.12.011.

Yamada, Masayuki, Akito Sone, Naonori Kuwabara, Kenji Ebisu, and Shuji Yamamoto. 2016. "Accurate Estimation of Strong Ground Motions and Simulation of Structural Damage At Kumamoto Port During the 2016 Kumamoto Earthquake," 1–12.

Yee, H C. 1987. "Construction of Explicit and Implicit Symmetric TVD Schemes and Their Applications." *Journal of Computational Physics* 68 (1): 151–79. https://doi.org/https://doi.org/10.1016/0021-9991(87)90049-0.

Yim, S. H.L., J. C.H. Fung, A. K.H. Lau, and S. C. Kot. 2009. "Air Ventilation Impacts of the 'Wall Effect' Resulting from the Alignment of High-Rise Buildings." *Atmospheric Environment* 43 (32): 4982–94. https://doi.org/10.1016/j.atmosenv.2009.07.002.